

PERIODIC VARIATIONS
OF THE
GRAVITATIONAL FORCE

Thesis by
Lloyd Philip Geldart

In Partial Fulfillment of the Requirements
For the Degree of
Geophysical Engineer

California Institute of Technology
Pasadena, California

1949

ACKNOWLEDGMENTS

The author wishes to express his gratitude to several persons who rendered valuable assistance in the work described in the following pages. The work involved in taking the readings, plotting the data, and calculating the gravity values was shared equally by Dr. C. Hewitt Dix, Mr. C. W. Faessler, and the author. R. Ingram, S. J., assisted greatly in carrying out the least squares calculations. In addition, the author wishes to acknowledge the valuable suggestions and guidance furnished by Dr. Dix under whose direction the project was carried out.

ABSTRACT

Using a La Coste and Romberg gravimeter, readings were taken every half hour for 72 hours immediately preceding full moon in the sub-basement of Mudd Building, California Institute of Technology, and for 56 hours immediately following in the interferometer building on Mount Wilson. Observed values were compared with values calculated on the hypothesis of a rigid earth, the results showing more yielding at Mount Wilson (22%) than at Mudd Building (16%). Effects due to ocean tides and barometric changes were estimated. After the removal of drift and earth tide effects, the residuals showed periods of 24, 12, 6, and 2 hours, the 24 hour period being very strong at Mount Wilson.

TABLE OF CONTENTS

<u>PART</u>	<u>TITLE</u>	<u>PAGE</u>
I	INTRODUCTION	1
II	THEORY OF THE TIDAL EFFECT	3
III	GRAPHICAL METHOD OF CALCULATING TIDAL EFFECT	9
IV	EXPERIMENTAL PROCEDURE	11
V	EXPERIMENTAL RESULTS	12
VI	DISCUSSION	14
VII	CONCLUSIONS	18
VIII	APPENDIX A: Pasadena Data	20
	Mount Wilson Data	23
IX	APPENDIX B: Theory of Least Squares	25
	Solution of Least Squares Equations	29
X	APPENDIX C: Calculation of Topographical Corrections	32
XI	REFERENCES	33

INTRODUCTION

It is well known that the gravitational force at a given point varies with time, the variations being due to changes in the attractive forces of the moon and sun as these bodies move relative to the earth. The amplitude of the effect is a function of the latitude of the observation point, and has a maximum value of about 0.3 mgls.

Because of the small magnitude of the variation, experimental measurements were not possible until sensitive measuring devices had been developed. Among the earliest observations are those of Schweydar (1), Hartsough (2), and Tomaschek and Schaffernicht (3). These workers used apparatus designed specially for measurements of the tidal variation. During the last twelve years commercial gravimeters have been used for this purpose by Wyckoff (4), Truman (5), Wolf (6), and Lockenvitz (7).

All of the measurements show that the amplitude of the observed effect is greater than the theoretical value for a perfectly rigid earth, but there is no agreement concerning the magnitude of the difference. Various observers have obtained values between eight and twenty per cent, while Lambert (8) estimates the value to be between ten and twenty per cent. A similar lack of agreement is evident with regard to the phase difference between the theoretical and observed curves, values between zero and 50' having been reported.

This disagreement between the different sets of data may result partly from the method of treating the data, for

example in allowing for drift, but it is probable that a considerable amount is due to variations in the rigidity of the earth, effects of ocean tides, barometric changes, etc. Since present-day gravimeters have been developed to the point where factors of this order of magnitude are important, any additional information which can be obtained is quite valuable.

During the course of the present experiment, a gravimeter was read at half-hour intervals for a period of approximately six days, from November 13 to 19, 1948. This period was chosen because the full moon, and therefore the maximum effect, occurred about midway during the period. During the first half of the period the instrument was set up in Room 0012 in the sub-basement of Mudd Building, California Institute of Technology. At the end of three days it was transferred to Mount Wilson where it was set up in the Interferometer Building and readings again taken for two and one half days.

Theoretical values of the tidal variation and the differences between corresponding theoretical and observed values were computed for the time of each observation. By making certain assumptions and using the methods of least squares, the components due to instrumental drift and to the non-rigidity of the earth were removed from the differences. In this way an estimate of the effect of the non-rigidity of the earth was obtained.

THEORY OF THE TIDAL EFFECT

Let g be the vertical component of the tidal gravitational force produced by a body m at the point P on the earth's surface, e and r being the distances from m to the point P and to the center of the earth respectively. Then assuming g to be positive when directed towards the center of the earth,

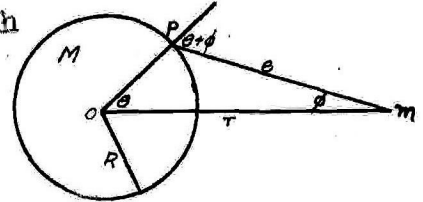


Fig. 1

$$g = -(km/e^2)\cos(\theta+\phi) + (km/r^2)\cos \theta ,$$

k being the gravitational constant.

If e and r are projected onto the line OP , then

$$e \cos(\theta+\phi) = r \cos \theta - R.$$

Using this relation to eliminate ϕ in the above, the following equation for g results.

$$\begin{aligned} g &= (km/r^2) [\cos \theta - (r^2/e^3)(r \cos \theta - R)] \\ &= (kM/R^2)(m/M)(R/r)^2 [\cos \theta - (r/e)^3(\cos \theta - R/r)] \\ &= G(m/M)q^2 [p - (p - q)(1 - 2pq + q^2)]^{-3/2} \end{aligned}$$

G being the gravitational field of the earth at P , $q = R/r$, $p = \cos \theta$, and e has been expressed in terms of p and q by means of the cosine law.

The quantity q is approximately $1/80$ for the moon, and $1/23,000$ for the sun; hence $(q^2 - 2pq) \ll 1$, and the right-hand bracket can be expanded by the binomial theorem.

$$g = G(m/M)q^2 \left[p - (p - q) \left\{ 1 - 3/2(q^2 - 2pq) + 15/8(q^2 - 2pq)^2 - 35/16(q^2 - 2pq)^3 + \dots \right\} \right]$$

$$g = G(m/M)q^3 \left[(1 - 3p^2) + q(9p/2 - 15p^3/2) + q^2(-3/2 + 15p^2 - 35/2p^4) + q^3(-75p/8 + 175p^3/4 - 315p^5/8) + \dots \right]$$

The coefficients of q^2 and q^3 inside the square bracket have their greatest numerical value when $p = \pm 1$. In the case of the moon, these values are approximately 0.001 and 0.00003, so that for 0.1% accuracy all terms in the square bracket involving powers of q higher than two can be neglected. For the sun q is so small that all terms inside the bracket involving q can be neglected.

Rewriting the expression for g in terms of p and using $1/60$ as the average value of q for the moon (inside the bracket only),

$$g = G(m/M)q^3 \left[(1 - 3p^2) + (-0.0004 + 0.0790p - 0.0042p^2 - 0.1248p^3 - 0.0049p^4) \right]$$

$$= 3G(m/M)q^3 \left[(1/3 - \cos^2\theta) + f(\theta) \right]$$

where $f(\theta) = 0.3533 \times 10^{-4} (-4 + 750 \cos \theta - 42 \cos^2 \theta - 1248 \cos^3 \theta - 49 \cos^4 \theta)$.

When the tidal effect of the sun is desired, the above formula with $f(\theta)$ set equal to zero can be used.

The quantity q depends upon the distance from the earth to the sun or moon, and can be expressed in terms of the equatorial horizontal parallax P as follows.

$$g = R/r = CR_{eq}/r = C \sin P$$

where R_{eq} is the equatorial radius of the earth, and C is a constant for a given point on the earth's surface. Using this expression for q , the formula for g becomes

$$g = 3G(m/M)C^3 \sin^3 P \left[(0.3533 - \cos^2\theta) + f(\theta) \right]$$

For the moon, P ranges from $54'$ to $61'$, and it is

convenient to write this formula in the following way.

$$g = 3G(m/M) (C \sin 60')^3 (\sin P / \sin 60')^3 [(0.3333 - \cos^2 \theta) + f(\theta)]$$

$$= K_m (\sin P / \sin 60')^3 [(0.3333 - \cos^2 \theta) + f(\theta)] \dots \dots (1)$$

The parallax of the sun changes much more slowly than that of the moon, and during the course of the present experiment it increased from 8.89" to 8.91". An average value of 8.90" was used for the entire period, thus introducing 0.3% error in the calculated effect of the sun during the first and last twelve hours of the experiment and a negligible error during the remainder of the period.

The constant C which appears in K_m can be calculated from the following equation for the figure of the earth (13).

$$R^2 = R_{eq}^2 [1 - (2e^2 - e^4) \sin^2 \phi] / (1 - e^2 \sin^2 \phi)$$

where $e = 0.08199$, and the latitude ϕ is $34^\circ 10'$. Using these values, $C = R/R_{eq} = 0.9989$.

The values of the remaining quantities appearing in K_m and the corresponding constant for the sun, K_s , are given below.

$$(m/M)_m = 0.01228 \quad (m/M)_s = 329,400 \quad G = 979.7 \text{ cm/sec}^2$$

With these values, it is found that $K_m = 0.1917$, $K_s = 0.0775$ when g is expressed in milligals. Substituting these values and adding the effects of the moon and sun, the final expression for g is obtained.

$$g = 0.1917 (\sin P / \sin 60')^3 [(0.3333 - \cos^2 \theta) + f(\theta)]_{\text{moon}}$$

$$+ 0.0775 [(0.3333 - \cos^2 \theta)]_{\text{sun}}$$

$$= 0.1917 (\sin P / \sin 60')^3 M(\theta) + 0.0775 S(\theta) \dots \dots (2)$$

The angle θ is not tabulated in the Ephemeris, and must be calculated from the declination and hour angle. In Fig. 2, page 7, $\delta = \text{AOM} = \text{declination}$, $H = \text{AOP} = \text{local hour angle}$, $\phi = \text{BOZ} = \text{latitude of the observer}$. Let OZ and Om be unit vectors, and take three mutually perpendicular unit vectors i, j, k along OB , the polar axis, and the normal to the plane of OB and OZ . Then,

$$\text{OZ} = (\cos \phi)i + (\sin \phi)j$$

$$\text{Om} = (\cos \delta \cos H)i + (\sin \delta)j - (\cos \delta \sin H)k$$

Since OZ and Om are unit vectors,

$$\cos \theta = \text{OZ} \cdot \text{Om} = \cos \delta \cos \phi \cos H + \sin \delta \sin \phi$$

The Greenwich hour angle of the moon and sun are tabulated for every ten minutes in the American Air Almanac, or they may be obtained from the American Ephemeris by subtracting the Right Ascension from the Sidereal Time and converting the answer from hours to angular measure. The local hour angle is found by subtracting the longitude of the point of observation from the Greenwich hour angle (adding for longitudes east of Greenwich).

The declination of both the sun and moon may be obtained from either of the above sources, along with the parallax of the moon. If the parallax of the sun is desired, it must be obtained from the Ephemeris.

The foregoing derivation of the tidal effect neglects several factors, and it is necessary to consider what errors might be introduced in this way. In addition to the vertical component, there is a horizontal component which is added

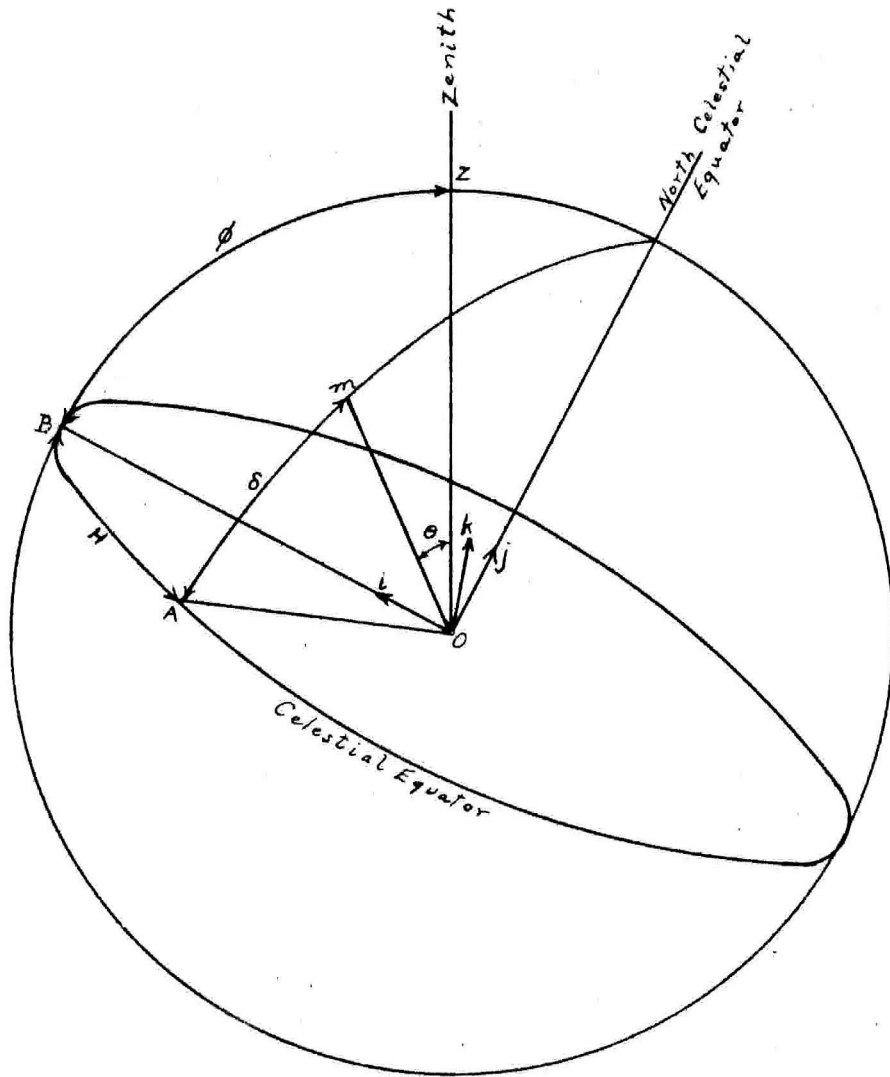


FIG. 2

vectorially to the total vertical component to give the resultant gravitational field. Since the horizontal component (g_h) is also a function of time, the direction of the resultant field varies. Thus, while the calculated values of the vertical component are along the radius vector from the center of the earth, measured values are along a line which oscillates about this direction. Referring to Fig. 1, page 3, the horizontal component is given by

$$\begin{aligned} g_h &= -(km/e^2)\sin(\theta+\phi) + (km/r^2)\sin \theta \\ &= (km/r^2) [1 - (r/e)^3] \sin \theta \end{aligned}$$

where the sine law has been used to eliminate ϕ . Proceeding as before it can be shown that

$$\begin{aligned} g_h &= -K_m(\sin P/\sin 60') \frac{1}{2}\sin 2\theta \quad \text{for the moon, and} \\ g_h &= -K_s \frac{1}{2}\sin 2\theta \quad \text{for the sun.} \end{aligned}$$

The maximum value of g_h is therefore $\frac{1}{2}(K_m + K_s)$, or 0.14 mgl. This is to be added to a vector perpendicular to g_h with a magnitude of approximately 980×10^3 mgl. This results in an inclination of the vertical by an angle whose tangent is 1.4×10^{-7} . To correct for this, the observed values should be multiplied by the cosine of this angle, that is, by $(1 - 0.98 \times 10^{-14})$. Therefore the effect is negligible.

The calculated value of g represents the component along the radius vector from the center of the earth to the point of observation, while the observed value is normal to the geoid. The angle ψ between these two directions is easily calculated in the following way.

The equation of an ellipse is $\rho^2 = a^2 b^2 / (a^2 \sin^2 \theta + b^2 \cos^2 \theta)$. The angle ϕ is given by $\tan \phi = \rho / \rho'$ where $\rho' = \frac{d\rho}{d\theta}$. Also, $\tan \phi = -\cot \psi$. Differentiating logarithmically,

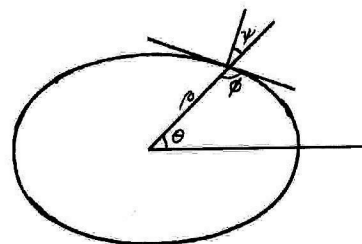


Fig. 3

$$-\tan \psi = \rho' / \rho = -(a^2 \sin \theta \cos \theta - b^2 \sin \theta \cos \theta) / (a^2 \sin^2 \theta + b^2 \cos^2 \theta) = (1 - e^2) / (\tan \theta + e^2 \cot \theta) \text{ where } e = b/a = 0.99664.$$

Substituting $\theta = 34^\circ 08'$, the latitude of Pasadena, ψ is found to be $10'48''$. Since $\cos 10'48'' = 0.99999$, this effect also contributes negligible error.

Formula 2, page 5, gives g as a function of P and θ where θ in turn is a function of the declination δ and the local hour angle H of the tide-producing body. The labor involved in calculating g from the formula for half-hour intervals over a period of six days would be tremendous, so graphical methods were used.

The accuracy of reading the gravimeter was ± 0.005 mg1, and therefore a graphical method of comparable accuracy was required. Adler (9) and Elkins (10) have described methods of graphical solution, but in both methods the accuracy is less than that required; therefore the method described in the following section was used.

GRAPHICAL METHOD OF CALCULATING THE TIDAL EFFECT

During the period of the experiment, the moon's declination increased from about 6°N to 28°N . Accordingly, tables were constructed for a latitude of $34^\circ 08' \text{N}$ and declinations of 5°N , 10°N , etc. up to 30°N . In the tables

were listed $\cos \theta$, $M(\theta)$, and $0.1917M(\theta)$ for 5° intervals of H from 0° to 360° . Graphs were plotted of $0.1917M(\theta)$ as a function of H for each value of δ .

Values of the moon's parallax were obtained from the Ephemeris for twelve hour intervals, and the parallax factor $(\sin P/\sin 60')^3$ plotted as a function of time.

A similar procedure was carried out for the sun, graphs of $S(\theta)$ for declinations of $18^\circ S$ and $20^\circ S$ only being required. No parallax correction was made in calculating the effect of the sun.

Copies of these curves will be found inside the back cover of the report.

The procedure for finding g is as follows:

(1) obtain the declinations and Greenwich hour angles of the moon and sun from the Air Almanac or Ephemeris for the required times, (2) obtain the parallax factor for the moon and the quantities $0.1917M(\theta)$ and $0.0775S(\theta)$ from the graphs, and add algebraically the product of the parallax factor and $0.1917M(\theta)$ to the quantity $0.0775S(\theta)$ - the result is g .

In computing the data used to plot the graphs, enough significant figures were used so that the final results were accurate to the nearest 0.0001 mgl. In addition, the accuracy of the graphs was checked by calculating g directly from the formula for several values of δ and H and comparing the values with those obtained from the graph. The maximum difference was 0.0003 mgl. Finally, all values obtained from the graphs were read twice, and it was found that readings were reprod-

ucible to within 0.0003 mgl. Since the maximum possible error in reading the gravimeter was 0.005 mgl, it is felt that the accuracy of values obtained by the graphical method was more than sufficient.

Tables similar to those described above were computed for Mount Wilson (latitude $34^{\circ}13'$) for declinations of $5^{\circ}N$ and $30^{\circ}N$, and it was found that the values differed from those for Pasadena (latitude $34^{\circ}08'$) by an amount which was usually less than 0.0001 mgl and had a maximum value of 0.0003 mgl when H was in the neighbourhood of 0° or 180° . Therefore the first set of curves was used for both places.

EXPERIMENTAL PROCEDURE

The instrument used for measuring the variations in gravity was a La Coste-Romberg gravimeter. The calibration was linear, each scale division being equal to 0.1011 mgl. In order to increase the sensitivity beyond the normal value, the instrument was adjusted so that it was off level by one minute. In order to minimize changes in sensitivity, the instrument was left unclamped during the entire period in which readings were being taken except for the interval during which it was being transported from Pasadena to Mount Wilson.

The level bubbles were checked at the time of each reading and did not deviate more than 0.2 minutes during the entire period. Preliminary tests showed that deviations of this magnitude were unimportant.

In order to increase the accuracy of reading the

scale, a small paper scale was added, the divisions of this scale being one tenth of the main divisions. In this way readings could be estimated to the nearest 0.05 divisions or 0.005 mgl. On some occasions microseisms reduced the accuracy of the readings to 0.2 divisions; this was particularly noticeable on Mount Wilson where the microseisms seem to be caused by moderate winds.

Backlash was avoided by always making the final adjustment with a clockwise rotation of the dial.

The instrument was first set up in Room 0012, Mudd Building, California Institute of Technology, and readings taken at intervals of one half hour from noon, November 13, until noon, November 16, 1948.. The instrument was then taken to Mount Wilson and set up in the Interferometer Building, and half hourly readings taken from 11.00 P.M., November 16, until 8.00 A.M., November 19. All times are Pacific Daylight Time. The data are listed in APPENDIX A, pages 20-24.

EXPERIMENTAL RESULTS

Using the graphical method already described, the theoretical value of g corresponding to each observed value was calculated, and both sets of values plotted as functions of time. The curves are inside the pocket at the back of the report. In order to have the curves superimposed, 0.850 mgl were subtracted from the values observed at Pasadena, and 0.400 mgl from the Mount Wilson values.

The differences (θ) between the observed values (g_o) and the calculated values (g_c) are listed in the tables in

APPENDIX A, and also plotted along with g_o and g_c .

As a first approximation it can be assumed that δ is made up of two parts: (1) a component due to drift of the instrument, the drift being a linear function of the time, (2) a part due to the non-rigidity of the earth. Love (11) has shown that the latter effect should be proportional to the theoretical value for a rigid earth. Hence δ was assumed to be of the form $\delta = kg_c + at + d$, where k , a , and d are constants, but have different values at Pasadena and Mount Wilson.

The method of least squares was used to obtain values of these constants for the two locations (the theory of the method and details of the calculations are given in APPENDIX B, pages 25-32). Substituting the values of these constants in the expression $\delta = (kg_c + at + d)$, and using the tabulated values of δ , g_c , and t , the differences (c_f) between the observed values of δ and the 'least squares best fit' value of δ can be calculated; also, as shown in APPENDIX B, the standard errors of the values of the constants can be found from the values of c_f and certain other data obtained in solving the least squares equations.

The constants k , a , and d , and the residuals c_f were calculated as well as the standard errors in k , a , and d . While the residuals c_f at Pasadena were small and more or less evenly distributed about the zero value, this was not so for the Mount Wilson data, and it was necessary to add a quadratic term to the drift. Therefore it was assumed that

$\phi = kg + ct^2 + at + d$. Using this expression, the values of k , c , a , d , and c_1 were calculated for the Mount Wilson data. The values obtained, together with the standard errors (except for the case of linear drift at Mount Wilson) are tabulated below.

	<u>Pasadena</u>	<u>Mount Wilson</u>	
		<u>Lin. Drift</u>	<u>Quad. Drift</u>
k	$(164 \pm 2) \times 10^{-3}$	341×10^{-9}	$(222 \pm 27) \times 10^{-8}$
d (mgl)	$(6507 \pm 2) \times 10^{-4}$	244×10^{-3}	$(188 \pm 6) \times 10^{-3}$
a (mgl/hr)	$(321 \pm 6) \times 10^{-6}$	640×10^{-5}	$-(120 \pm 4) \times 10^{-4}$
c (mgl/hr ²)			$-(105 \pm 9) \times 10^{-6}$

DISCUSSION

Examination of the curves for Pasadena shows the following: (1) except for small irregularities, the curve of g_0 is almost an exact replica of the curve of g_c ; (2) there is no observable phase shift, both g_0 and g_c reaching their extreme values at the same times; (3) the amplitude of the g_0 curve is greater than that of the g_c curve.

The Mount Wilson curves of g_0 and g_c also resemble one another but to a much smaller degree. The g_0 curves are more irregular, and as a result it is not possible to draw definite conclusions regarding phase shift, although if a phase difference does exist, it is less than about one hour, that is, less than 15 degrees. Furthermore, the g_0 curve shows very clearly the effect of a large instrumental drift which is very likely a result of clamping the instrument and transporting it to Mount Wilson.

The amplitude of the g_0 curves is roughly 15-25% greater than the amplitude of the g_c curves, the difference ϕ

corresponding to a value of k between 16.2 and 16.6% at Pasadena and 19.5 to 24.9% at Mount Wilson. Since these two ranges of values do not overlap, it seems reasonable to conclude that there is a significant difference between the two sets of data, and that this difference is probably related to variations in the effective rigidity of the earth.

If ϕ were entirely the result of non-rigidity, then according to Love's theory (11), the ϕ curves should be small scale copies of the g_c curves, and the values of $c_p^!$ should have a random distribution about the value zero. Obviously the ϕ curves bear only a very general resemblance to the g_c curves, and the $c_p^!$ curves have a pronounced periodicity, periods of six, twelve, and twenty-four hours (with some indications of a two hour period) being evident. Moreover, the maximum amplitude of the $c_p^!$ curves is roughly 0.030 to 0.040 mg1 which is between six and eight times the error in reading the instrument. It is evident therefore that, while a part of the residuals $c_p^!$ is undoubtedly the result of random errors, a considerable portion must result from effects omitted in the least-squares treatment.

The effect of non-rigidity has been taken into account by assuming a linear relation between the tidal forces and the observed gravity value, that is, $\phi = kg_c + d$ (except for drift). This assumption is open to considerable question, since the relation between these two quantities is by no means a simple one. As a result of the non-rigidity

the surface of the earth moves under the influence of the tidal forces. This produces two effects on the force of gravity, one resulting from the variation in the distance from the point to the center of the earth, and the other resulting from the acceleration of the gravimeter. Since the phase difference between the g_0 and g_c curves is small, it seems probable that the acceleration is very nearly in phase with the tidal forces. Assuming the two to be in phase, then the acceleration at any instant should be proportional to g_c . Disregarding the effect of changes in parallax, g_c may be written $g_c = K - k_m \cos^2 \theta_m - k_s \cos^2 \theta_s$ (see page 5), K , k_m , and k_s being constants. The displacement of the earth is obtained by integrating this expression twice, and it is obvious that the result will not be proportional to g_c . Also it is known that the amplitude of the earth tide is about three or four inches (14) which corresponds to 0.02 mg1 (using the free air correction). Thus the effect of the displacement may contribute a considerable amount to the non-rigidity effect, and if there is appreciable phase difference between the displacement and acceleration the departures from the assumed linear relation between δ and g_c will be even greater.

In addition to earth tides, changes in the barometric pressure and ocean tides affect the force of gravity. This effect is a result of the attraction of the mass added or removed, together with the acceleration and displacement of the surface of the earth resulting from the change in mass

distribution. No data is available which would permit the calculation of the effects of acceleration and displacement, but the approximate value of the maximum attraction in each case can be estimated as follows.

In the case of the atmosphere, a first approximation can be obtained by considering it to be made up of an infinite number of parallel plane laminae of constant surface density, the laminae extending to infinity in all directions. Changes in the barometric pressure are equivalent to the addition or subtraction of laminae with surface density dm . The attraction of such a lamina at a given point is $4\pi\gamma dm$, γ being the gravitational constant; thus the attraction is independent of the distance between the given point and the lamina. The change in attraction resulting from a change in barometric pressure, P , is given by $\int 4\pi\gamma dm = 4\pi\gamma\Delta P$, ΔP being in gm/cm^2 . Multiplying by 1.02 to convert ΔP to millibars, and substituting the value of γ , the change in gravity is equal to $0.00085\Delta P$ mgl. During the course of the experiment the difference between the highest and lowest barometric pressures was about 10 mb which corresponds to 0.0085 mgl.

The method of calculating the attraction of the ocean tide is the same as that used for making topographical corrections; the details of the method are given in APPENDIX C. The results obtained were 0.000024h mgl at Pasadena and 0.00014h mgl at Mount Wilson, h being the height of the tide in feet. From tidal data supplied by the United States Coast and Geodetic Survey at Los Angeles, it was found that

the maximum difference between high and low tide during the course of the experiment was seven feet. This gives a correction of 0.0002 mgl at Pasadena and 0.0010 mgl at Mount Wilson.

Since the maximum change in gravity resulting from these two factors combined cannot exceed 0.0100 mgl, while c_r^1 changes from about -0.4 mgl to +0.4 mgl, it is obvious that these attractive forces alone cannot account for c_r^1 . At the same time, it is quite possible that these forces, along with the effects of the displacements and accelerations, may make a very considerable contribution to the residuals.

In order to show relative periods and amplitudes, curves of the barometric pressure, ocean tide at Los Angeles (approximate only), ϕ , and c_r^1 have been plotted above one another (see inside of back cover).

CONCLUSIONS

The differences in the results obtained at the two locations, particularly with regard to k , may be related to many factors, for example, the differences in geologic structure and rock types in the upper layers of the crust, changes in instrumental drift as a result of moving the instrument, large variations in the order of magnitude of the random error, perhaps as a result of the higher rate of incidence of microseisms at Mount Wilson. The effects of these various factors could be minimized or separated by taking simultaneous readings with more than one instrument, preferably a large number, the readings being taken in areas of different geologic structure,

and at various distances from the ocean.

Another improvement would be to use the least squares method to eliminate as far as possible the effect of the ocean tides and barometric changes.

Finally, a harmonic analysis of the residuals should throw some light upon their origin, as well as permit an estimate of the magnitudes of the various components.

- 20 -
APPENDIX A: Pasadena Data

Nov. 13

Nov. 14

Time (PDT)	t	So (div)	So (mg/l)	Sc (mg/l)	Ø (mg/l)	Ø _{least Sq} (mg/l)	c† (mg/l)
12.00	0.00	6.20	0.6268	-0.0266	0.6534	0.6463	+0.0071
12.30	0.50	6.25	0.6319	-0.0174	0.6493	0.6480	+0.0013
13.00	1.00	6.40	0.6470	-0.0054	0.6524	0.6501	+0.0023
13.30	1.50	6.50	0.6572	+0.0082	0.6490	0.6525	-0.0035
14.00	2.00	6.65	0.6723	+0.0225	0.6498	0.6550	-0.0052
14.30	2.50	6.75	0.6824	+0.0363	0.6461	0.6574	-0.0113
15.00	3.00	6.90	0.6976	+0.0493	0.6483	0.6597	-0.0114
15.30	3.50	7.05	0.7128	+0.0598	0.6530	0.6616	-0.0086
16.00	4.00	7.15	0.7229	+0.0670	0.6559	0.6629	-0.0070
16.30	4.50	7.15	0.7229	+0.0709	0.6520	0.6637	-0.0117
17.00	5.00	7.15	0.7229	+0.0703	0.6526	0.6638	-0.0112
17.30	5.50	7.10	0.7178	+0.0649	0.6529	0.6631	-0.0102
18.00	6.00	7.05	0.7128	+0.0553	0.6575	0.6617	-0.0042
18.30	6.50	6.90	0.6976	+0.0419	0.6557	0.6596	-0.0039
19.00	7.00	6.75	0.6824	+0.0258	0.6566	0.6571	-0.0005
19.30	7.50	6.55	0.6622	+0.0065	0.6557	0.6541	+0.0016
20.00	8.00	6.35	0.6420	-0.0132	0.6552	0.6511	+0.0041
20.30	8.50	6.20	0.6268	-0.0341	0.6609	0.6454	+0.0155
21.00	9.00	5.95	0.6015	-0.0542	0.6557	0.6446	+0.0111
21.30	9.50	5.80	0.5864	-0.0713	0.6577	0.6420	+0.0157
22.00	10.00	5.65	0.5712	-0.0861	0.6573	0.6397	+0.0176
22.30	10.50	5.50	0.5561	-0.0970	0.6531	0.6381	+0.0150
23.00	11.00	5.40	0.5459	-0.1037	0.6496	0.6372	+0.0124
23.30	11.50	5.35	0.5409	-0.1058	0.6467	0.6370	+0.0097
24.00	12.00	5.45	0.5510	-0.1028	0.6538	0.6376	+0.0162
00.30	12.50	5.50	0.5561	-0.0957	0.6518	0.6389	+0.0129
01.00	13.00	5.65	0.5712	-0.0831	0.6543	0.6412	+0.0131
01.30	13.50	5.95	0.6015	-0.0680	0.6695	0.6438	+0.0257
02.00	14.00	6.15	0.6218	-0.0500	0.6718	0.6469	+0.0249
02.30	14.50	6.40	0.6470	-0.0294	0.6764	0.6504	+0.0260
03.00	15.00	6.55	0.6622	-0.0088	0.6710	0.6540	+0.0170
03.30	15.50	6.70	0.6774	+0.0105	0.6669	0.6573	+0.0096
04.00	16.00	6.85	0.6925	+0.0279	0.6646	0.6603	+0.0043
04.30	16.50	7.00	0.7077	+0.0432	0.6645	0.6630	+0.0015
05.00	17.00	7.10	0.7178	+0.0557	0.6621	0.6652	-0.0031
05.30	17.50	7.25	0.7330	+0.0634	0.6696	0.6666	-0.0030
06.00	18.00	7.40	0.7481	+0.0667	0.6663	0.6673	-0.0010
06.30	18.50	7.40	0.7481	+0.0658	0.6823	0.6673	+0.0150
07.00	19.00	7.30	0.7380	+0.0605	0.6775	0.6666	+0.0109
07.30	19.50	7.15	0.7229	+0.0527	0.6702	0.6652	+0.0050
08.00	20.00	7.00	0.7077	+0.0417	0.6660	0.6638	+0.0022
08.30	20.50	6.75	0.6824	+0.0296	0.6528	0.6620	-0.0092
09.00	21.00	6.55	0.6622	+0.0160	0.6462	0.6599	-0.0137
09.30	21.50	6.35	0.6420	+0.0031	0.6389	0.6580	-0.0191
10.00	22.00	6.20	0.6268	-0.0079	0.6347	0.6563	-0.0216
10.30	22.50	6.10	0.6167	-0.0167	0.6334	0.6550	-0.0216
11.00	23.00	6.05	0.6117	-0.0214	0.6331	0.6544	-0.0213
11.30	23.50	6.00	0.6066	-0.0242	0.6308	0.6541	-0.0233
12.00	24.00	6.00	0.6066	-0.0227	0.6293	0.6545	-0.0252
12.30	24.50	6.05	0.6117	-0.0169	0.6286	0.6556	-0.0270
13.00	25.00	6.15	0.6218	-0.0079	0.6297	0.6573	-0.0276
13.30	25.50	6.35	0.6420	+0.0051	0.6369	0.6596	-0.0227
14.00	26.00	6.60	0.6673	+0.0169	0.6504	0.6617	-0.0113
14.30	26.50	6.80	0.6875	+0.0308	0.6567	0.6641	-0.0074
15.00	27.00	7.00	0.7077	+0.0444	0.6633	0.6665	-0.0032
15.30	27.50	7.20	0.7279	+0.0566	0.6713	0.6686	+0.0027
16.00	28.00	7.40	0.7481	+0.0657	0.6824	0.6703	+0.0121

Nov. 14

Nov. 15

Time (PDT)	t	g_0 (μ v)	g_0 (mg/l)	g_c (mg/l)	θ (mg/l)	$\theta_{\text{Least Sq}}$ (mg/l)	c_t (mg/l)
16.30	28.50	7.45	0.7532	+0.0723	0.6809	0.6715	+0.0094
17.00	29.00	7.45	0.7532	+0.0742	0.6790	0.6720	+0.0070
17.30	29.50	7.40	0.7481	+0.0719	0.6762	0.6718	+0.0044
18.00	30.00	7.30	0.7380	+0.0646	0.6734	0.6707	+0.0027
18.30	30.50	7.25	0.7330	+0.0533	0.6797	0.6690	+0.0107
19.00	31.00	7.15	0.7229	+0.0381	0.6848	0.6667	+0.0181
19.30	31.50	6.85	0.6925	+0.0192	0.6733	0.6638	+0.0095
20.00	32.00	6.60	0.6673	-0.0021	0.6694	0.6604	+0.0090
20.30	32.50	6.20	0.6268	-0.0243	0.6511	0.6570	-0.0059
21.00	33.00	5.90	0.5965	-0.0473	0.6438	0.6533	-0.0095
21.30	33.50	5.65	0.5712	-0.0682	0.6394	0.6501	-0.0107
22.00	34.00	5.45	0.5510	-0.0878	0.6388	0.6470	-0.0082
22.30	34.50	5.15	0.5207	-0.1029	0.6236	0.6447	-0.0211
23.00	35.00	5.00	0.5055	-0.1154	0.6209	0.6428	-0.0219
23.30	35.50	4.90	0.4954	-0.1220	0.6174	0.6419	-0.0245
24.00	36.00	4.85	0.4903	-0.1235	0.6138	0.6418	-0.0280
00.30	36.50	4.95	0.5004	-0.1195	0.6199	0.6426	-0.0227
01.00	37.00	5.15	0.5207	-0.1102	0.6309	0.6443	-0.0134
01.30	37.50	5.40	0.5459	-0.0971	0.6430	0.6466	-0.0036
02.00	38.00	5.70	0.5763	-0.0797	0.6560	0.6496	+0.0064
02.30	38.50	6.00	0.6066	-0.0593	0.6659	0.6531	+0.0128
03.00	39.00	6.25	0.6319	-0.0370	0.6689	0.6569	+0.0120
03.30	39.50	6.60	0.6673	-0.0143	0.6816	0.6608	+0.0208
04.00	40.00	6.75	0.6824	+0.0081	0.6743	0.6646	+0.0097
04.30	40.50	6.85	0.6925	+0.0281	0.6644	0.6681	-0.0037
05.00	41.00	7.15	0.7229	+0.0460	0.6769	0.6712	+0.0057
05.30	41.50	7.30	0.7380	+0.0601	0.6779	0.6736	+0.0043
06.00	42.00	7.50	0.7583	+0.0690	0.6893	0.6752	+0.0141
06.30	42.50	7.55	0.7633	+0.0742	0.6891	0.6763	+0.0128
07.00	43.00	7.60	0.7684	+0.0742	0.6942	0.6764	+0.0178
07.30	43.50	7.60	0.7684	+0.0708	0.6976	0.6760	+0.0216
08.00	44.00	7.55	0.7633	+0.0640	0.6993	0.6751	+0.0242
08.30	44.50	7.40	0.7481	+0.0532	0.6949	0.6734	+0.0215
09.00	45.00	7.20	0.7279	+0.0409	0.6870	0.6716	+0.0154
09.30	45.50	7.05	0.7128	+0.0279	0.6849	0.6696	+0.0153
10.00	46.00	6.90	0.6976	+0.0152	0.6824	0.6677	+0.0147
10.30	46.50	6.65	0.6723	+0.0044	0.6679	0.6661	+0.0018
11.00	47.00	6.50	0.6572	-0.0051	0.6623	0.6647	-0.0024
11.30	47.50	6.45	0.6521	-0.0104	0.6625	0.6640	-0.0015
12.10	48.16	6.45	0.6521	-0.0125	0.6646	0.6638	+0.0008
12.30	48.50	6.45	0.6521	-0.0110	0.6631	0.6642	-0.0011
13.00	49.00	6.50	0.6572	-0.0063	0.6635	0.6651	-0.0016
13.30	49.50	6.50	0.6572	+0.0024	0.6548	0.6667	-0.0119
14.00	50.00	6.70	0.6774	+0.0130	0.6644	0.6686	-0.0042
14.30	50.50	6.85	0.6925	+0.0259	0.6666	0.6709	-0.0043
15.00	51.00	7.00	0.7077	+0.0391	0.6686	0.6732	-0.0046
15.30	51.50	7.10	0.7178	+0.0520	0.6658	0.6755	-0.0097
16.00	52.00	7.15	0.7229	+0.0628	0.6601	0.6774	-0.0173
16.30	52.50	7.20	0.7279	+0.0716	0.6563	0.6790	-0.0227
17.00	53.00	7.25	0.7330	+0.0764	0.6566	0.6799	-0.0233
17.30	53.50	7.15	0.7229	+0.0774	0.6455	0.6802	-0.0347
18.00	54.00	7.05	0.7128	+0.0732	0.6396	0.6797	-0.0401
18.30	54.50	7.05	0.7128	+0.0608	0.6520	0.6778	-0.0258
19.00	55.00	7.05	0.7128	+0.0516	0.6612	0.6765	-0.0153
19.30	55.50	7.00	0.7077	+0.0350	0.6727	0.6739	-0.0012
20.00	56.00	6.80	0.6875	+0.0141	0.6734	0.6707	+0.0027

Time (PDT)	t	S_0 (div)	S_0 (mg/l)	S_c (mg/l)	ϕ (mg/l)	$\phi_{Least Sq}$ (mg/l)	c-f (mg/l)
20.30	56.50	6.50	0.6572	-0.0088	0.6660	0.6671	-0.0011
21.00	57.00	6.25	0.6319	-0.0330	0.6649	0.6632	+0.0017
21.30	57.50	6.00	0.6066	-0.0576	0.6642	0.6594	+0.0048
22.00	58.00	5.80	0.5864	-0.0795	0.6659	0.6559	+0.0100
22.30	58.50	5.60	0.5662	-0.0995	0.6657	0.6528	+0.0129
23.00	59.00	5.25	0.5308	-0.1207	0.6515	0.6496	+0.0019
23.30	59.50	5.10	0.5156	-0.1282	0.6438	0.6484	-0.0046
24.00	60.00	5.05	0.5106	-0.1353	0.6459	0.6474	-0.0015
00.30	60.50	5.10	0.5156	-0.1369	0.6525	0.6473	+0.0052
01.00	61.00	5.10	0.5156	-0.1324	0.6480	0.6482	-0.0002
01.30	61.50	5.25	0.5308	-0.1234	0.6542	0.6498	+0.0044
02.00	62.00	5.40	0.5459	-0.1091	0.6550	0.6523	+0.0027
02.30	62.50	5.60	0.5662	-0.0907	0.6569	0.6555	+0.0014
03.00	63.00	6.00	0.6066	-0.0689	0.6755	0.6592	+0.0163
03.30	63.50	6.25	0.6319	-0.0458	0.6777	0.6632	+0.0145
04.00	64.00	6.50	0.6572	-0.0216	0.6788	0.6673	+0.0115
04.30	64.50	6.60	0.6673	+0.0022	0.6651	0.6714	-0.0063
05.00	65.00	6.90	0.6976	+0.0245	0.6731	0.6752	-0.0021
05.30	65.50	7.20	0.7279	+0.0410	0.6839	0.6785	+0.0054
06.00	66.00	7.25	0.7330	+0.0592	0.6738	0.6812	-0.0074
06.30	66.50	7.55	0.7633	+0.0702	0.6931	0.6832	+0.0099
07.00	67.00	7.70	0.7785	+0.0768	0.7017	0.6844	+0.0173
07.30	67.50	7.75	0.7835	+0.0792	0.7043	0.6850	+0.0193
08.00	68.00	7.75	0.7835	+0.0770	0.7065	0.6847	+0.0218
08.30	68.50	7.65	0.7734	+0.0711	0.7023	0.6839	+0.0184
09.00	69.00	7.50	0.7583	+0.0621	0.6962	0.6826	+0.0136
09.30	69.50	7.20	0.7279	+0.0509	0.6770	0.6809	-0.0039
10.00	70.00	7.10	0.7178	+0.0388	0.6790	0.6791	-0.0001
10.30	70.50	6.85	0.6925	+0.0268	0.6657	0.6773	-0.0116
11.00	71.00	6.80	0.6875	+0.0158	0.6717	0.6757	-0.0040
11.30	71.50	6.70	0.6774	+0.0073	0.6701	0.6744	-0.0043
12.00	72.00	6.50	0.6572	+0.0018	0.6554	0.6737	-0.0183

Note: $\phi_{Least Sq}$ in the tables on pages 20-24 is the value of ϕ obtained from the least-squares values of k, a, c, and d.

- 23 -
Mount Wilson Data

Time (P.D.T)	t	t ²	R ₀	R ₁	R ₂	φ	φ _{Least Sq}	c ₁
			(div)	(mgls)	(mgls)	(mgls)	(mgls)	(mgls)
Nov. 16	23.00	0.00	1.15	0.1163	-0.1062	0.2225	0.1654	+0.0571
23.30	0.50	0.25	0.50	0.0505	-0.1234	0.1739	0.1677	+0.0062
24.00	1.00	1.00	0.40	0.0404	-0.1354	0.1758	0.1710	+0.0048
00.30	1.50	2.25	0.35	0.0354	-0.1430	0.1784	0.1753	+0.0031
01.00	2.00	4.00	0.30	0.0303	-0.1447	0.1750	0.1809	-0.0059
01.30	2.50	6.25	0.45	0.0455	-0.1406	0.1863	0.1876	-0.0013
02.00	3.00	9.00	0.60	0.0607	-0.1318	0.1925	0.1954	-0.0029
02.30	3.50	12.25	0.80	0.0809	-0.1184	0.1993	0.2041	-0.0048
03.00	4.00	16.00	1.05	0.1062	-0.0996	0.2058	0.2140	-0.0082
03.30	4.50	20.25	1.40	0.1415	-0.0782	0.2197	0.2244	-0.0047
04.00	5.00	25.00	1.70	0.1719	-0.0544	0.2263	0.2353	-0.0090
04.30	5.50	30.25	2.05	0.2073	-0.0314	0.2387	0.2460	-0.0073
05.00	6.00	36.00	2.40	0.2426	-0.0061	0.2487	0.2571	-0.0084
05.30	6.50	42.25	2.50	0.2528	+0.0166	0.2362	0.2675	-0.0313
06.00	7.00	49.00	2.75	0.2780	+0.0369	0.2411	0.2774	-0.0363
06.30	7.50	56.25	3.00	0.3033	+0.0534	0.2499	0.2864	-0.0365
07.00	8.00	64.00	3.25	0.3286	+0.0662	0.2624	0.2946	-0.0322
07.30	8.50	72.25	3.40	0.3437	+0.0743	0.2694	0.3016	-0.0322
08.00	9.00	81.00	3.50	0.3538	+0.0782	0.2756	0.3077	-0.0321
08.30	9.50	90.25	3.55	0.3589	+0.0782	0.2807	0.3128	-0.0321
09.00	10.00	100.00	3.60	0.3640	+0.0738	0.2902	0.3169	-0.0267
09.30	10.50	110.25	3.60	0.3640	+0.0666	0.2974	0.3203	-0.0229
10.00	11.00	121.00	3.60	0.3640	+0.0574	0.3066	0.3232	-0.0166
10.30	11.50	132.25	3.55	0.3589	+0.0470	0.3119	0.3258	-0.0139
11.00	12.00	144.00	3.60	0.3640	+0.0363	0.3277	0.3283	-0.0006
11.30	12.50	156.25	3.65	0.3690	+0.0265	0.3425	0.3310	+0.0115
12.00	13.00	169.00	3.60	0.3640	+0.0187	0.3453	0.3340	+0.0113
12.40	13.67	186.87	3.65	0.3690	+0.0121	0.3569	0.3388	+0.0181
13.00	14.00	196.00	3.75	0.3791	+0.0107	0.3684	0.3416	+0.0268
13.30	14.50	210.25	3.80	0.3842	+0.0118	0.3724	0.3464	+0.0260
14.00	15.00	225.00	3.90	0.3943	+0.0156	0.3787	0.3518	+0.0269
14.30	15.50	240.25	4.05	0.4095	+0.0222	0.3873	0.3578	+0.0295
15.00	16.00	256.00	4.20	0.4246	+0.0309	0.3937	0.3642	+0.0295
15.30	16.50	272.25	4.40	0.4448	+0.0410	0.4038	0.3708	+0.0330
16.00	17.00	289.00	4.60	0.4651	+0.0519	0.4132	0.3776	+0.0356
16.30	17.50	300.25	4.75	0.4802	+0.0629	0.4173	0.3849	+0.0324
17.00	18.00	324.00	4.95	0.5004	+0.0712	0.4292	0.3904	+0.0388
17.30	18.50	342.25	5.05	0.5106	+0.0773	0.4333	0.3959	+0.0374
18.00	19.00	361.00	5.10	0.5156	+0.0801	0.4355	0.4007	+0.0348
18.30	19.50	380.25	5.15	0.5207	+0.0792	0.4415	0.4046	+0.0369
19.00	20.00	400.00	5.15	0.5207	+0.0738	0.4469	0.4074	+0.0395
19.30	20.50	420.25	4.95	0.5004	+0.0641	0.4363	0.4092	+0.0271
20.00	21.00	441.00	4.70	0.4752	+0.0497	0.4255	0.4099	+0.0156
20.30	21.50	462.25	4.60	0.4651	+0.0318	0.4333	0.4098	+0.0235
21.00	22.00	484.00	4.35	0.4398	+0.0104	0.4294	0.4089	+0.0205
21.30	22.50	506.25	4.15	0.4196	-0.0128	0.4324	0.4075	+0.0249
22.00	23.00	529.00	3.85	0.3892	-0.0374	0.4266	0.4058	+0.0208
22.30	23.50	552.25	3.55	0.3589	-0.0618	0.4207	0.4040	+0.0167
23.00	24.00	576.00	3.25	0.3286	-0.0848	0.4134	0.4025	+0.0109
23.30	24.50	600.25	3.00	0.3033	-0.1054	0.4087	0.4015	+0.0072
24.00	25.00	625.00	2.70	0.2730	-0.1225	0.3955	0.4012	-0.0057
Nov. 18	00.30	25.50	2.55	0.2578	-0.1362	0.3940	0.4016	-0.0076
01.00	26.00	676.00	2.50	0.2528	-0.1437	0.3965	0.4033	-0.0068
01.30	26.50	702.25	2.55	0.2578	-0.1464	0.4042	0.4061	-0.0019
02.00	27.00	729.00	2.60	0.2629	-0.1441	0.4070	0.4099	-0.0029
02.30	27.50	756.25	2.70	0.2730	-0.1360	0.4090	0.4149	-0.0059

Time (PDT)	t	t ²	g _o (dwt)	g _o (mg ls)	g _c (mg ls)	ϕ (mg ls)	ϕ _{Least Sq.} (mg ls)	c† (mg ls)
03.00	28.00	784.00	2.85	0.2881	-0.1235	0.4116	0.4209	-0.0093
03.30	28.50	812.25	3.10	0.3134	-0.1071	0.4205	0.4276	-0.0071
04.00	29.00	841.00	3.30	0.3336	-0.0864	0.4200	0.4353	-0.0153
04.30	29.50	870.25	3.55	0.3589	-0.0643	0.4232	0.4432	-0.0200
05.00	30.00	900.00	3.95	0.3993	-0.0406	0.4399	0.4515	-0.0116
05.30	30.50	930.25	4.10	0.4145	-0.0171	0.4316	0.4596	-0.0280
06.00	31.00	961.00	4.35	0.4398	+0.0053	0.4345	0.4675	-0.0330
06.30	31.50	992.25	4.60	0.4651	+0.0257	0.4394	0.4748	-0.0354
07.00	32.00	1024.00	4.85	0.4903	+0.0428	0.4475	0.4814	-0.0339
07.30	32.50	1056.25	5.15	0.5207	+0.0562	0.4645	0.4871	-0.0226
08.00	33.00	1089.00	5.20	0.5257	+0.0665	0.4592	0.4920	-0.0328
08.30	33.50	1122.25	5.25	0.5308	+0.0726	0.4582	0.4960	-0.0378
09.00	34.00	1156.00	5.25	0.5308	+0.0743	0.4565	0.4989	-0.0424
09.30	34.50	1190.25	5.25	0.5308	+0.0722	0.4586	0.5010	-0.0424
10.00	35.00	1225.00	5.30	0.5358	+0.0677	0.4681	0.5024	-0.0343
10.30	35.50	1260.25	5.35	0.5409	+0.0611	0.4798	0.5033	-0.0235
11.00	36.00	1296.00	5.30	0.5358	+0.0528	0.4830	0.5038	-0.0208
11.30	36.50	1332.25	5.25	0.5308	+0.0443	0.4865	0.5042	-0.0177
12.00	37.00	1369.00	5.25	0.5308	+0.0359	0.4949	0.5046	-0.0097
12.30	37.50	1406.25	5.25	0.5308	+0.0288	0.5020	0.5052	-0.0032
13.00	38.00	1444.00	5.25	0.5308	+0.0230	0.5078	0.5068	+0.0010
13.30	38.50	1482.25	5.30	0.5358	+0.0218	0.5140	0.5079	+0.0061
14.00	39.00	1521.00	5.35	0.5409	+0.0221	0.5188	0.5100	+0.0088
14.30	39.50	1560.25	5.45	0.5510	+0.0245	0.5265	0.5125	+0.0140
15.00	40.00	1600.00	5.55	0.5611	+0.0299	0.5312	0.5156	+0.0156
15.30	40.50	1640.25	5.70	0.5763	+0.0371	0.5392	0.5191	+0.0201
16.00	41.00	1681.00	5.85	0.5914	+0.0454	0.5460	0.5229	+0.0231
16.30	41.50	1722.25	5.95	0.6015	+0.0551	0.5464	0.5267	+0.0197
17.00	42.00	1764.00	6.10	0.6167	+0.0636	0.5531	0.5303	+0.0228
17.30	42.50	1806.25	6.20	0.6268	+0.0708	0.5560	0.5336	+0.0224
18.00	43.00	1849.00	6.25	0.6319	+0.0760	0.5559	0.5363	+0.0196
18.30	43.50	1892.25	6.15	0.6218	+0.0785	0.5433	0.5384	+0.0049
19.00	44.00	1936.00	6.15	0.6218	+0.0769	0.5449	0.5396	+0.0053
19.30	44.50	1980.25	6.05	0.6117	+0.0718	0.5399	0.5399	+0.0000
20.00	45.00	2025.00	5.90	0.5965	+0.0622	0.5343	0.5392	+0.0049
20.30	45.50	2070.25	5.80	0.5864	+0.0494	0.5370	0.5377	+0.0007
21.00	46.00	2116.00	5.70	0.5763	+0.0325	0.5438	0.5352	+0.0086
21.30	46.50	2162.25	5.50	0.5560	+0.0125	0.5435	0.5320	+0.0115
22.00	47.00	2209.00	4.85	0.4903	-0.0439	0.5342	0.5224	+0.0118
22.30	47.50	2256.25	4.80	0.4853	-0.0594	0.5407	0.5204	+0.0203
23.00	48.00	2304.00	4.80	0.4853	-0.0594	0.5407	0.5204	+0.0203
23.30	48.50	2352.25	4.45	0.4499	-0.0772	0.5271	0.5166	+0.0105
24.00	49.00	2401.00	4.15	0.4196	-0.0975	0.5171	0.5131	+0.0040
00.30	49.50	2450.25	3.85	0.3892	-0.1151	0.5043	0.5101	-0.0058
01.00	50.00	2500.00	3.80	0.3842	-0.1281	0.5123	0.5081	+0.0042
01.35	50.58	2558.34	3.60	0.3640	-0.1386	0.5026	0.5067	-0.0041
02.00	51.00	2601.00	3.55	0.3589	-0.1420	0.5009	0.5066	-0.0057
02.30	51.50	2652.25	3.45	0.3488	-0.1408	0.4896	0.5076	-0.0180
03.35	52.58	2764.66	3.75	0.3791	-0.1225	0.5016	0.5130	-0.0114
04.00	53.00	2809.00	4.00	0.4014	-0.1107	0.5151	0.5161	-0.0010
04.35	53.58	2870.82	4.25	0.4297	-0.0905	0.5202	0.5211	-0.0009
05.00	54.00	2916.00	4.40	0.4488	-0.0736	0.5384	0.5253	+0.0131
06.00	55.00	3025.00	5.15	0.5207	-0.0299	0.5506	0.5357	+0.0149
06.30	55.50	3080.25	5.30	0.5358	-0.0090	0.5448	0.5407	+0.0041
07.40	56.67	3211.49	5.80	0.5864	+0.0339	0.5525	0.5507	+0.0018

Nov. 18

Nov. 19

APPENDIX B

THE THEORY OF LEAST SQUARES

The following account of the theory of least squares is the one given by Jeffreys (12). Jeffreys bases his theory upon a theorem known as Bayes' principle of inverse probability. Using the notation $P(q|p)$ for the probability of the proposition q given the proposition p , the theorem may be stated thus: $P(q_r|p,H) = kP(q_r|H)P(p|q_r,H)$ where k is the quantity $1/P(p|H)$, and q_r is any one of the propositions or sets of data q_1, q_2, q_3 , etc. Thus, if q_r represents a set of data, then $P(q_r|H)$ is the probability of these data on a given set of hypotheses H . Then, if p is a further set of hypotheses or data, $P(p|q_r,H)$ is the probability of p on q_r and H , and $P(q_r|p,H)$, which is the probability of q_r given p and H , is proportional to the product of the probabilities of q_r given H and that of p given q_r and H .

The normal law of errors may be written in the form

$$P(dx|H) = (1/\sqrt{2\pi}\sigma) \exp \left[-(x-p)^2 / 2\sigma^2 \right] dx ,$$

where $P(dx|H)$ is the probability that the measured value x of a quantity whose true value is p will lie between x and $x+dx$, σ being the standard error. In a least-squares problem there are m unknowns, x_i , and n sets of data to determine the values of x , n being greater than m . The problem is to determine the set of values of the x_i 's which gives the best solution of the problem.

Let c_r represent sets of data, n in number, so that

$$c_r = f_r(x_1, x_2, \dots, x_n), \quad r = 1, 2, \dots, n,$$

provided there is no random error. Because of these errors, however, this equation must be replaced by the probability relation $P(dc_r | x_1, \sigma, H) = (1/\sqrt{2\pi}\sigma) \exp[-(c_r - f_r)^2 / 2\sigma^2] dc_r$

Assume that the errors in the observations are independent, also that the standard error σ is known. If \emptyset represents all of the observations, then the probability that the values of the c_r 's will lie between c_1 and $c_1 + dc_1$, c_2 and $c_2 + dc_2$, etc. is $P(\emptyset | x_1, \sigma, H)$ where

$P(\emptyset | x_1, \sigma, H) = \left[1 / (2\pi\sigma^2)^{n/2} \right] \exp \left[-S(c_r - f_r)^2 / 2\sigma^2 \right] dc_1 dc_2 \dots dc_n$, where S denotes summation with respect to the n observations.

In most practical cases, the function f_r is linear in the unknowns x_1 , that is, $f_r = \sum_{i=1}^m a_{ir} x_i = a_{ir} x_i$, adopting the convention that repetition of a suffix indicates summation with respect to that suffix from 1 to m .

$$\begin{aligned} \text{Let } W &= \frac{1}{2} S(c_r - f_r)^2 = \frac{1}{2} S(c_r - a_{ir} x_i)^2 \\ &= \frac{1}{2} S(c_r^2 - 2a_{ir} c_r x_i + a_{ir} a_{jr} x_i x_j) \\ &= \frac{1}{2} b_{ij} x_i x_j - d_i x_i + \frac{1}{2} S c_r^2 \quad \text{where } b_{ij} = S a_{ir} a_{jr} \end{aligned}$$

and $d_i = S a_{ir} c_r$. It can be shown that there is a unique set of values of the x_1 's for which W is a minimum, and it is assumed that these values are the best values of the unknown. Let y_i be these values of x_i , so that the y_i 's are the roots of the equations obtained by differentiating W with respect to each of the x_i 's and equating each of the expressions to zero. These equations are linear in x_i and are of the form

$$b_{ij} y_j - d_i = 0.$$

The equations for y_j have a unique solution if $m < n$ and the determinant b_{ij} is not zero. Write $x_i = y_i + z_i$,

and $c_r' = c_r - a_{ir}y_i$, where c_r' is a residual, that is, the difference between the observed value of c_r and the value calculated from the least squares values of the x_i 's. W can be expressed in terms of the z_i 's and the residuals as follows.

$$\begin{aligned} W &= \frac{1}{2}b_{ij}x_ix_j - d_1x_1 + \frac{1}{2}Sc_r^2 \\ &= \frac{1}{2}b_{ij}z_iz_j + \frac{1}{2}b_{ij}y_iy_j + b_{ij}z_iz_j - d_1(y_1 + z_1) + \frac{1}{2}Sc_r^2 \\ &= \frac{1}{2}b_{ij}z_iz_j + (\frac{1}{2}b_{ij}y_iy_j - d_1y_1 + \frac{1}{2}Sc_r^2) + z_1(b_{ij}y_j - d_1) \\ &= \frac{1}{2}b_{ij}z_iz_j + \frac{1}{2}S(a_{ir}y_i - c_r)^2 \text{ since } (b_{ij}y_j - d_1) = 0 \\ &= \frac{1}{2}b_{ij}z_iz_j + \frac{1}{2}Sc_r^2 . \end{aligned}$$

The quantity $b_{ij}z_iz_j$ is equal to $S(a_{ir}z_i)^2$ and therefore is essentially positive. It can be reduced to a sum of m squares in the following way. Consider the case where $i, j = 1, 2, 3$. Then, if $F = b_{ij}z_iz_j$,

$$F = b_{11}z_1^2 + 2b_{12}z_1z_2 + b_{22}z_2^2 + 2b_{13}z_1z_3 + 2b_{23}z_2z_3 + b_{33}z_3^2.$$

This can be written

$$F - b_{11}Q_1^2 = b_{22}z_2^2 + 2b_{23}z_2z_3 + b_{33}z_3^2$$

where $Q_1 = z_1 + (b_{12}z_2 + b_{13}z_3)/b_{11}$, $b_{ij}' = b_{ij} - b_{1i}b_{1j}/b_{11}$.

Next take $Q_2 = z_2 + (b_{23}z_3)/b_{22}$. Then

$$F - b_{11}Q_1^2 - b_{22}Q_2^2 = b_{33}''z_3^2, \text{ and}$$

$$F = b_{11}Q_1^2 + b_{22}Q_2^2 + b_{33}''Q_3^2,$$

where $Q_3 = z_3$, and $b_{ij}'' = b_{ij}' - b_{1i}'b_{1j}'/b_{22}'$.

In the Jacobian $\frac{\partial(Q_1, \dots, Q_m)}{\partial(z_1, \dots, z_m)}$ all the diagonal terms are one, and all terms to one side of the diagonal are zero, since $\partial Q_i / \partial z_j = 0$ for $i > j$. Thus the Jacobian has the value one, and $dz_1 dz_2 \dots dz_m = dx_1 dx_2 \dots dx_m$ can be replaced by $dQ_1 dQ_2 \dots dQ_m$.

If it is assumed that the priori probabilities of z_1, z_2, \dots, z_m are uniformly distributed, then, when σ is known and is the same for all of the z_i 's,

$$P(dz_1, dz_2, \dots, dz_m | \sigma, H) \propto dz_1 dz_2 \dots dz_m$$

Also, $P(dz_1, dz_2, \dots, dz_m | \sigma, H, \emptyset) \propto dz_1 dz_2 \dots dz_m P(\emptyset | \sigma, H)$ using the principle of inverse probability. Therefore,

$$P(dz_1, dz_2, \dots, dz_m | \sigma, H, \emptyset) \propto \sigma^{-n} \exp(-W/\sigma^2) dz_1 dz_2 \dots dz_m \\ \propto \sigma^{-n} \exp[-(b_1 Q_1^2 + Sc_r'^2)/2\sigma^2] dz_1 dz_2 \dots dz_m$$

where b_1 is used in place of b_{11} . This expression breaks up into factors which depend upon only one of the Q_i 's, so that for any one of the Q_i 's

$$P(dQ_i | \sigma, H, \emptyset) \propto (1/\sqrt{2\pi b_i} \sigma^2) \exp(-b_i Q_i^2 / 2\sigma^2) dQ_i$$

Hence the standard error of Q_i is $\sigma/\sqrt{b_i}$, and since $Q_m = z_m$, the standard error in z_m is $\sigma/\sqrt{b_m}$. However,

$x_m = y_m + z_m$, and the true value of z_m is zero. Therefore z_m is equal to the standard error in z_m , and accordingly,

$$x_m = y_m \pm \sigma/\sqrt{b_m}. \text{ Similarly, for any } x_i, x_i = y_i \pm \sigma/\sqrt{b_i}.$$

If σ is unknown, then (Cf. Jeffreys, page 115)

$$P(dQ_1 \dots dQ_m, d\sigma | H) \propto dQ_1 \dots dQ_m d\sigma / \sigma$$

$$P(dQ_1 \dots dQ_m, d\sigma | \emptyset, H) \propto \sigma^{-n} \exp[-(b_1 Q_1^2 + Sc_r'^2)/2\sigma^2] dQ_1 \dots dQ_m d\sigma / \sigma$$

Integrating with respect to all of the Q_i 's except Q_m , between the limits $-\infty$ and $+\infty$,

$$P(dQ_m, d\sigma | \emptyset, H) \propto \sigma^{-n+n-2} \exp[-(b_m Q_m^2 + Sc_r'^2)/2\sigma^2] dQ_m d\sigma$$

Integrating next with respect to σ from 0 to ∞ ,

$$P(dQ_m | \emptyset, H) \propto (b_m Q_m^2 + Sc_r'^2)^{-(n-m+1)/2} dQ_m \\ \propto (1 + b_m Q_m^2 / Sc_r'^2)^{-(n-m+1)/2} dQ_m.$$

Thus Q_m follows the t distribution with $(n-m)$ degrees of freedom. Hence, if $(n-m)$ is large, the distribution is approximately normal with a standard error $\sigma_m = S c_r^2 / (n-m) \sqrt{b_m}$.

SOLUTIONS OF THE LEAST-SQUARES EQUATIONS.

Using the data tabulated in APPENDIX A, the following values are obtained.

Pasadena

$Sg_1 = -8.99$	$Sg_1^2 = 5668.1857$	$Sg_1 t_1 = -365.559$
$St_1 = 5220.4$	$St_1^2 = 251472.88$	$Sg_1 \phi_1 = 87.29115$
$S\phi_1 = 89.843$	$N = 145$	$S\phi_1 t_1 = 3433.8452$

(S denotes summation with respect to the N observations; also in order to simplify the calculations, ϕ has been replaced by $\phi' = 10(\phi - 0.6000)$ and g_1 has been expressed in units of 10^{-2} mg/l. The g_1 values are the calculated values denoted in the preceding pages by s_c).

Mount Wilson

$Sg_1 = -113.83$	$Sg_1^2 = 6706.2953$	$Sg_1 \phi_1 = -24.429375$
$S\phi_1 = 45.7035$	$St_1^2 = 110909$	$Sg_1 t_1 = -3051.327500$
$St_1 = 3012.0$	$St_1^3 = 4610016$	$Sg_1 t_1^2 = -185450.228$
$N = 110$	$St_1^4 = 204988833$	$S\phi_1 t_1 = 1433.748375$
		$S\phi_1 t_1^2 = 55356.107169$

(g_1 is in units of 10^{-2} mg/l).

Solution for Pasadena

Assuming a linear drift (see page 13), the expression

$$S[\phi_1 - (kg_1 + at_1 + d)]^2$$

is to be a minimum. Differentiating the above expression

with respect to k, a, and d in turn and equating each result to zero, the following equations are obtained.

$$(Sg_1^2)k + (Sg_1 t_1)a + (Sg_1)d = S\phi_1 g_1 \dots \dots \dots (1)$$

$$(Sg_1 t_1)k + (St_1^2)a + (St_1)d = S\phi_1 t_1 \dots \dots \dots (2)$$

$$(Sg_1)k + (St_1)a + Nd = S\phi_1 \dots \dots \dots (3)$$

Substituting the data tabulated on the preceding page,

$$5668.1857k - 365.559a - 8.99d = 87.29115 \dots \dots (1)$$

$$-365.559k + 251472.88a + 5220.4d = 3433.8452 \dots \dots (2)$$

$$-8.99k + 5220.4a + 145d = 89.843 \dots \dots (3)$$

k is eliminated by dividing (1) by 5668.1857, then multiplying the result by -365.559 and -8.99 in turn, and subtracting the equations obtained from (2) and (3) respectively. This gives the following equations.

$$251449a + 5219.820d = 3439.47 \dots \dots \dots (2a)$$

$$5219a + 144.986d = 89.98 \dots \dots \dots (3a)$$

a is eliminated next by multiplying equation (2a) by the quantity 5219/251449 and subtracting the result from (3a). This leads to the result

$$36.6278d = 18.5816$$

$$d = 0.507, b_d = 36.6$$

To obtain a and b_a the original equations are re-written so that a is the last unknown on the left-hand side and the equation obtained by differentiating with respect to a is the last equation. This is accomplished by interchanging the terms involving d and a, and also equations (2) and (3). These equations are solved as above, and the process repeated a third time to obtain k and b_k. The final results

are listed below.

$$k = 0.0164 \qquad a = 0.00321 \qquad d = 0.507$$

$$b_k = 5670 \qquad b_a = 63000 \qquad b_d = 36.6$$

Since $\phi_1 = 10(\phi_1 - 0.6000)$, the least squares value of ϕ_1 is $0.1\phi_1 + 0.6000 = 0.1(0.0164g_1 + 0.00321t_1 + 0.507) + 0.6000$.

Therefore the residuals, c_1 , are given by

$$\begin{aligned} c_1 &= \phi_1 - 0.00164g_1 - 0.000321t_1 - 0.6507, \quad g_1 \text{ in units of } 10^{-2} \text{ mgl,} \\ &= \phi_1 - 0.164g_1 - 0.000321t_1 - 0.6507, \quad g_1 \text{ being in mgl.} \end{aligned}$$

The values of the residuals were found by substituting in this expression, the values being listed in APPENDIX A.

The sum of the squares of the residuals is 0.0279.

The standard error, σ_s , is given by (see page 29)

$$\begin{aligned} \sigma_s^2 &= \sum_{i=1}^N c_1^2 / (N-m)b_s \\ &= 0.0002b_s \end{aligned}$$

Therefore, $k = (164 \pm 2) \times 10^{-4}$, $a = (321 \pm 6) \times 10^{-5}$, $d = (507 \pm 2) \times 10^{-3}$ when g_1 is in units of 10^{-2} mgl and ϕ' is used, and

$k = (164 \pm 2) \times 10^{-3}$, $a = (321 \pm 6) \times 10^{-6}$, $d = (6507 \pm 2) \times 10^{-4}$ when g_1 is in mgl and ϕ is used.

Solution for Mount Wilson

For the case of linear drift, solution of the three equations by the method outlined in the preceding section gives the following values (g_1 being in mgl).

$$k = 0.341 \qquad a = 0.00640 \qquad d = 0.244$$

The values of the standard errors were not calculated.

For the case where the drift is assumed to be of the form $ct_1^2 + at_1 + d$, the following results were obtained.

$$\begin{array}{lll} k = (222 \pm 27) \times 10^{-3} & a = (120 \pm 4) \times 10^{-4} & c = -(105 \pm 9) \times 10^{-6} \\ b_k = 5690 & b_a = 3030 & b_c = 5,290,000 \\ d = (188 \pm 6) \times 10^{-3} & b_d = 11.6 & Sc_1^2 = 0.0480 \end{array}$$

APPENDIX C

Calculation of Topographical Corrections

The topographical correction for a given body may be calculated by dividing the body up into thin segments bounded by horizontal planes. The vertical component of gravity at a point P produced by one of these thin laminae may be calculated from the following formula

$$g = \rho \gamma h \int \frac{d\theta}{r}$$

where ρ is the density, γ the gravitational constant, h the height of the lamina above P, Δh the thickness of the lamina, $d\theta$ the angle subtended at P by an element of the curve bounding the lamina, and r the distance from this element to P. The integral is taken around the entire curve bounding the segment.

In practice a topographical map may be used, the segments being defined by the contour lines. The values of the integral are then found by numerical integration.

REFERENCES

- (1) Schweydar, W.: Sita. Ber. der Preuss. Akad. d. Wiss.,
Math. phys., Kl. 14, 454 (1914).
- (2) Hartsough, R. C.: Phys., Rev., 19, 282 (1922).
- (3) Tomaschek and Schaffernicht: Ann. der Phys., XV, 787 (1932).
- (4) Wyckoff, R. D.: Trans. Am. Geophys. Union, 17th annual
meeting, pp. 46-52 (1936).
- (5) Truman, O. H.: Astrophys. Jour., 89, 445 (1939).
- (6) Wolf, A.: Geophysics, 5, 317 (1940).
Geophysics, 6, 81 (1941).
- (7) Lockenvitz, A. E.: Geophysics, 9, 94 (1944).
- (8) Lambert, W. D.: Geophysics, 8, 51 (1943).
Report on Earth Tides, 1936-38, U.S.C.
and G. S., Spec. Publ. No. 223.
- (9) Adler, J. L.: Geophysics, 7, 35 (1942).
- (10) Elkins, T. A.: Geophysics, 8, 134 (1943).
- (11) Love, A. E. H.: Some Problems of Geodynamics (Cambridge
University Press), pp. 52-54 (1911).
- (12) Jeffreys, H.: The Theory of Probability (Oxford University
Press), second Edition, pp. 129-135.
- (13) Smart, W. M.: Spherical Astronomy (Cambridge
Univ. Press), pp. 197-198 (1947)
- (14) Lambert, W. D.: Bull. of the National Research
Council, No. 78, p. 71 (1931).

A GRAVITY SURVEY IN THE
MONK HILL AREA

Thesis by
Lloyd Philip Geldart

In Partial Fulfillment of the Requirements
For the Degree of
Geophysical Engineer

California Institute of Technology
Pasadena, California
1949

ACKNOWLEDGMENTS

The author wishes to express his gratitude to Dr. C. Hewitt Dix, California Institute of Technology, for his valuable guidance and advice in connection with the work described in this report.

ABSTRACT

Using a La Coste and Romberg gravimeter, gravity values were obtained at 65 stations in the vicinity of Monk Hill, Pasadena. A density value for elevation corrections was obtained using a least squares method and data obtained with a network of 35 stations in Washington Park. A topographical correction was also made for the San Gabriel Mountains to the north of the area.

The corrected gravity data were used to calculate elevations of the basement along Howard Street, and the resulting basement profile compared with one obtained by a seismograph survey.

TABLE OF CONTENTS

<u>PART</u>	<u>TITLE</u>	<u>PAGE</u>
I	INTRODUCTION	1
II	GEOLOGY OF THE RAYMOND BASIN	2
III	EXPERIMENTAL PROCEDURE	4
IV	DENSITY DETERMINATION	5
V	TREATMENT OF THE DATA	8
VI	INTERPRETATION OF THE DATA	11
VII	CONCLUSIONS	16
VIII	APPENDIX A: Gravity Data for Monk Hill Area	18
IX	APPENDIX B: Survey Data for Washington Park	21
	Gravity Data for Washington Park	22
	Data for Determination of Density	23
	Least Squares Determination of k	24
X	REFERENCES	25

A GRAVITY SURVEY OF THE MONK HILL AREA, PASADENA, CALIFORNIA.

INTRODUCTION

The Raymond Basin is a structural basin, roughly triangular in shape, and bounded on the north by the San Gabriel Mountains, on the west and southwest by the San Rafael Hills, on the east by the Monrovia Hills, and on the south by low hills and scarps along the Raymond Fault. The topography of the basin is quite irregular, and in places basement rocks project above the surface of the alluvium which fills most of the basin. Monk Hill is formed by one of these projections, and rises about 200 feet above the level of the surrounding alluvium.

Data obtained from numerous wells in the area indicate that the water table immediately north of Monk Hill is roughly 300 feet higher than the water table just south of the hill. This is a matter of considerable economic importance, and several investigations have been carried out with the object of determining the causes of this abrupt change in gradient of the water table. Previous investigations include a geologic survey by Dr. J. P. Buwalda of the Division of Geological Sciences, California Institute of Technology, seismic work by the Geophysical Engineering Corporation, and an electrical survey by R. W. Lehman. None of the results of these investigations have been published, but the author had access to all three reports.

Since the alluvium in the basin is continuous and relatively

permeable, the flow of subsurface water will depend to a large extent upon the topography of the floor of the basin. For this reason, it was felt that a gravity survey of the area should yield important additional information. Unfortunately, lack of time did not permit the carrying out of as extensive a survey as had been planned originally, and the data are therefore incomplete.

GEOLOGY OF THE RAYMOND BASIN.

The basin is traversed by four major faults, the Raymond, Eagle Rock, Linda Vista, and Sierra Madre Faults. These are reverse faults dipping steeply towards the north, and trending roughly east-west. The basin itself is the result of vertical movements along these faults, the fault blocks having been rotated downwards towards the north, and to a much lesser extent downwards towards the east. Although there is some evidence of motion along these faults in Quaternary times, most of the displacements were probably pre-Quaternary.

The floor of the basin is quite irregular with a maximum relief of several hundreds of feet. Prior to the deposition of the alluvium, a drainage system was established on bedrock, the principal valleys being those of the old Arroyo Seco, along with its tributary valley, the La Canada Valley. These valleys were probably located in roughly the same positions as their present-day counterparts. There is considerable evidence for the existence of a third valley just east of Monk Hill, this valley being much shallower than the others and trending roughly northwest-southeast.

Surface data as well as the seismic data indicate that a ridge of bedrock probably extends eastward from the northeast part of the San Rafael Hills, Monk Hill being a high point on this ridge. This ridge, if it exists, could account for the sudden change in gradient of the water table in this vicinity, since a large part of the subsurface water would be forced to flow through gorges cut in the ridge by the old Arroyo Seco and other ancient streams.

The San Gabriel Mountains to the north and the San Rafael Hills to the west are composed largely of old crystalline rocks, mainly metasediments with some intrusions of granite and other types of igneous rocks (1). Since all the outcrops of the basin floor, including those on Monk Hill, are of these same rock types, it is probable that the entire floor is largely crystalline meta-sediments.

Presumably most of the basin is filled with Quaternary alluvium derived mainly from the San Gabriel area; however, the possibility that parts of the basin contain other sediments cannot be ruled out since Tertiary sandstones, shales, and conglomerates outcrop in the southwest portion of the basin. The alluvium ranges in size from clay to large boulders, sand to gravel sizes being most common in the central area. The alluvium is largely acidic in composition, and was derived mainly from granite, diorite, schist, and gneiss. Streams issuing from the San Gabriel Mountains deposited the alluvium in the form of coalescing fans which slope gently southward. The alluvium is poorly indurated and therefore is quite porous and permeable relative to the crystalline rocks and Tertiary sediments.

EXPERIMENTAL PROCEDURE

Gravity values were obtained at 65 stations in an area of approximately 0.6 square miles around Monk Hill. Four north-south profiles were run along Raymond, Summit, Marengo, and Garfield Avenues, extending from Montana Street in the north to Mountain Street in the south. One east-west profile was run along Howard Street from Fair Oaks Avenue in the east to Arroyo Boulevard in the west. In addition, three of the stations in the vicinity of Washington Park which were read in the course of the density determination were plotted on the gravity map.

The instrument used was a La Coste-Romberg gravimeter, the sensitivity being 0.1011 milligals per scale division. Readings could be estimated to within 0.2 scale divisions, that is, to within 0.02 milligals. The effects of tidal variations and instrumental drift were reduced to a minimum by taking check readings at a fixed station at intervals of thirty or forty minutes. Each profile was connected with a preceding profile by including one or more stations of the latter with the former. All stations, except those used in determining the density, were located at bench marks established by the Engineering Department of the City of Pasadena. The locations of the stations are shown on the accompanying map (see inside of back cover).

To obtain a density value for elevation corrections, a network of 35 evenly distributed stations was set up in Washington Park, about one-half mile east of Monk Hill. The coordinates and elevations of these stations were determined by a compass-and-stadia survey, the

horizontal coordinates being accurate to within about three or four feet, and the elevations to within 0.2 feet.

In running the profiles, the meter was transported in a car, since all the bench marks were located on the curbs. In Washington Park, however, it was necessary to carry the meter or else use a small cart, and on several occasions it was found that slight jarring of the meter resulted in large changes in the drift rate. For this reason, it was necessary to read each station twice, and in some cases three times.

DENSITY DETERMINATION

J. A. Legge (2) has given the theory of a least-squares method of obtaining the density from data obtained with an areal distribution of stations. Let x_i , y_i , z_i , and g_i be respectively the two coordinates in a horizontal plane, the elevation above a given datum plane, and the acceleration of gravity at the i^{th} station. Then the value of g_i corrected to the datum plane is

$$G_i = g_i + kz_i,$$

k being a function of the density and having the same value for all stations.

It is assumed furthermore that the corrected values G_i can be expressed as a polynomial of the coordinates x_i , y_i , so that

$$G_i = \sum_{r=0}^{r=m} \sum_{s=0}^{s=n} a_{rs} x_i^r y_i^s.$$

If the stations are located on a straight line which may be taken to be the X axis, and if G_i varies linearly, then

$$G_i = a_0 + a_1 x_i.$$

When the stations are distributed throughout an area, and if it is assumed that $G_i(x_i, y_i)$ defines a plane, then

$$G_i = a_{00} + a_{10}x_i + a_{01}y_i \dots \dots \dots (1)$$

The following discussion will deal only with this case, but the results for the linear case can be obtained merely by omitting all terms which involve y_i .

G_i can be eliminated from (1) by using the relation

$$G_i = g_i + kz_i \text{ giving the equation}$$

$$(a_{00} + a_{10}x_i + a_{01}y_i) - (g_i + kz_i) = 0 \dots \dots \dots (2)$$

In this equation there are four unknowns, since x_i , y_i , z_i , and g_i are measured quantities. Therefore a unique solution can be obtained if data for four stations are known. However, to obtain a higher degree of accuracy, more data must be used; in this case the resulting equations no longer have a unique solution, and the method of least squares is used to obtain the values of the constants which give the best fit.

The theory of least squares requires that the quantity

$$\sum_{i=1}^N [(a_{00} + a_{10}x_i + a_{01}y_i) - (g_i + kz_i)]^2 \dots \dots \dots (3)$$

(N being the number of stations) be a minimum for variations of a_{00} , a_{10} , a_{01} , and k . Differentiating the expression with respect to each of these in turn, and equating the results to zero, four equations are obtained from which the values of the four unknowns can be found. To simplify the writing of the equations, the convention is adopted that wherever a suffix is repeated, summation from 1 to N with respect to that suffix is indicated. Thus,

$x_{ii} = \sum_{i=1}^N x_i, x_i y_i = \sum_{i=1}^N x_i y_i$. The four equations may now be written

$$\begin{aligned} a_{00}N + a_{10}x_{ii} + a_{01}y_{ii} - kz_{ii} &= \delta_{ii} \\ a_{00}x_{ii} + a_{10}x_{ii}^2 + a_{01}y_i x_i - kz_i x_i &= \delta_i x_i \\ a_{00}y_{ii} + a_{10}x_i y_i + a_{01}y_{ii}^2 - kz_i y_i &= \delta_i y_i \quad \dots \dots (4) \\ -a_{00}z_{ii} - a_{10}x_i z_i - a_{01}y_i z_i + kz_{ii}^2 &= -\delta_i z_i \end{aligned}$$

These equations can be solved by the determinant method, but it was found from experience that it was less laborious to solve for k by elimination. This has an added advantage in that it furnishes automatically part of the data required to obtain a value of the standard error of k. This is discussed in detail in the report on Periodic Variations of the Gravitational Force (see the section on Theory of Least Squares), where it is shown that k and the standard error, σ_k , can be determined by the following procedure. Equations (4) are solved by dividing the first equation by N, and multiplying the result by x_{ii} , y_{ii} , and $-z_{ii}$ in turn, then subtracting these three equations from the second, third and fourth equations of (4) respectively. In this way a_{00} is eliminated; the same procedure is repeated to eliminate a_{10} , then a_{01} , care being taken to keep the equations in the proper order. The final result is an equation in k only. Let the coefficient of k in this equation be b_k . The values of a_{00} , a_{10} , a_{01} are found by the usual method, and the values of the four unknowns substituted in (3). When the values of x_i , y_i , z_i , δ_i for each station are substituted in (3), a quantity, c_i^2 , is obtained. Then the standard error in k is given by the relation $\sigma_k^2 = (\sum_{i=1}^N c_i^2)/(N-4) b_k \dots \dots \dots (5)$

TREATMENT OF THE DATA

The data used in determining the density are listed in Tables 1, 2, and 3, Appendix B, pages 21-23. The details of the calculation of k and b_k are set forth on page 24, immediately following the tables. The values obtained for k and b_k are 0.680 div/ft or 0.0687 mg1/ft, and 1,074 respectively. The residuals, c_i , were calculated (see Table 3, page 23) and the sum of the squares, $\sum_{i=1}^N c_i^2$, was found to be 4.83. Substituting this value in Eqn. (5) above, along with the values of N and b_k , σ_k is found to be 0.012. Using twice the standard error, $k = 0.680 \pm 0.024$ div/ft, or 0.0687 ± 0.0024 mg1/ft., where the probability is approximately one in twenty that if k were redetermined in the same area a value lying outside this range would be obtained (3).

The elevation factor k is a combination of the free-air and Bouguer corrections, and is equal to $(-0.09406 + 0.01276\rho)$ mg1/ft, ρ being the density of the surface layers. The above value of k corresponds to $\rho = 1.98 \pm 0.24$ gm/cm³.

The data for the stations in the Monk Hill area are listed in APPENDIX A, pages 18-20. The gravimeter readings were converted to milligals by multiplying by the factor 0.1011 after which corrections were applied for drift, elevation, latitude variation, and topography.

The correction for drift was obtained by plotting the readings taken at the check stations and reading from the graph corrections to be applied to each observation. These corrections were adjusted so that the proper gravity values were obtained for at least one station

occupied in a previous survey.

The elevation correction was calculated using $k = 0.0687$ mgl/ft and a datum level of 900 feet above sea level. The elevations given in APPENDIX A refer to this same datum plane.

The variation of gravity with latitude was allowed for in the following manner. From the International Formula, $g = 978.049(1 + 5.2884 \times 10^{-3} \sin^2 \phi)$, ϕ being the latitude. Taking the Y axis in the north direction, then

$$\begin{aligned} dg/dy &= (1/R)dg/d\phi \\ &= 1.3068 \sin 2\phi \text{ mgl/mile.} \end{aligned}$$

The area covered by the survey extended from latitude $34^{\circ} 10' N$ to $34^{\circ} 12' N$, hence the average value of the variation is $1.3068 \sin 68^{\circ} 22' = 1.210$ mgl/mile. Also, $d(dg/dy) = 2.61 \cos 2\phi d\phi = 0.0005$ mgl/mile using $d\phi = 2'$. Therefore no appreciable error is introduced by using an average value over the area.

A topographical correction for the San Gabriel Mountains to the north of the area was calculated in the following manner. A topographical map with a scale of 1:250,000 and 500-foot contour intervals was used to calculate the effect of the mountains at each of two points in the survey area, one point being 1.55 miles due north of the other. The details of the method of calculation are described in the report on Periodic Variations of the Gravitational Force, page 32. The values 3.73 and 2.71 milligals were obtained for the two points which correspond to a gradient of 0.658 mgl/mile in the north-south direction. Since the axis of the mountains is roughly east-west

in this region, the east-west component of the gradient was neglected. Moreover, since the surface of the ground is relatively flat in the vicinity of Monk Hill, no other topographical corrections were made.

Under the above assumptions, the topographical correction is linear, and depends only upon the north-south coordinate. Thus, it can be combined with the latitude correction giving a combined correction coefficient of 0.552 mg1/mile or 0.0104 mg1/100 ft (the corrections have opposite signs and must be subtracted). If the correction is taken to be zero at a given point, then it will be negative for stations north of this point and positive for stations south of the point.

Washington Street extends east-west in this area, and therefore the south side of the street was chosen as a reference line for the combined latitude-topographical correction. Distances north or south of this line are listed in the tables in APPENDIX A in the column headed 'y' (a plus sign is used for stations north of the reference line and a minus sign for stations south of the line). The combined correction is also given in the same tables under the heading 'Lat.' Corr.

The gravimeter readings were corrected for drift, elevation, latitude variation, and topography as described above, the corrected gravity readings being listed in APPENDIX A in the column headed 'g'. These values were plotted on the map of the area (see inside of back cover), and contour lines drawn.

INTERPRETATION OF THE DATA

Since the basement rocks are relatively denser than the alluvium, the gravity contours should reflect the basement topography in a very general way. Although only a limited number of contours could be drawn because of the small number of stations, nevertheless the data are consistent with the above statement since the pronounced high about one half block south of the intersection of Howard and Marengo Avenue coincides almost exactly with the highest point of Monk Hill.

A profile was drawn along Howard street (see inside back cover), and a rough estimate of the depth of the basement obtained by the following procedure.

The vertical component of the attraction of a point mass is given by the expression (referring to Fig. 1)

$$\begin{aligned} g &= (\gamma m/r^2) \cos \phi = (\gamma m/z^2) \cos^3 \phi \\ &= g_0 \cos^3 \phi \end{aligned}$$

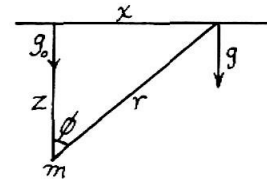


Fig. 1

The resulting curve for g as a function of x has a maximum at $x = 0$, g being equal to g_0 at this point, and there are two points of inflection symmetrically placed with respect to the point $x = 0$, the distance between the two points of inflection being equal to z .

This expression was used to determine a series of point masses which would give a curve similar to Curve A. Both positive and negative masses were used, negative masses corresponding to depressions in the basement, and therefore to minima on Curve A.

As a first approximation, a single negative point mass with a g_0 value of 2 mgl was used, the depth being 3000 feet (roughly the distance between the points of inflection of Curve A). The values of g were readily obtained by dividing x by 3000 to obtain $\tan \phi$, then using a table of natural trigonometric functions to obtain $\cos \phi$ from the value of $\tan \phi$; cubing $\cos \phi$ and multiplying by 2 gives g . It was found that this point mass gave a very poor fit, and examination of the two curves suggested using two shallower point masses.

After some trial and error calculations, it was found that one positive and one negative mass, both with g_0 equal to 1 mgl, gave a good fit. The negative mass is under the intersection of Howard and El Sereno at a depth of 1800 feet (below the datum plane); the positive mass is 1200 feet below a point 100 feet east of the intersection of Howard and Marengo. Curve B was obtained by subtracting algebraically the combined effects of these masses from Curve A.

Curve b is relatively flat in the central portion, rises steadily near the western end, and has a sharp bump near the eastern end. The steady rise in the western part is very likely a result of a gradual thinning of the alluvium near Arroyo Boulevard as shown by outcrops on the east bank of the Arroyo Seco. This part of the curve is neglected in the following discussion, since there are insufficient data to justify any calculations regarding it.

Further smoothing of curve B was accomplished by assuming two additional masses, the first with a g_0 value of 0.7 mgl and 600 feet below a point on Howard Street midway between Raymond and Marengo Avenues, the second with a g_0 value of 0.2 mgl and 400 feet below

the intersection of Howard Street and Raymond Avenue. Subtracting the effects of these masses gives Curves C and D, respectively.

The total force of gravity produced by these four point masses was subtracted from the gravity contours in the Monk Hill area. This was accomplished by drawing concentric circles about the positions of the various masses, the circles representing gravity contours in the datum plane at intervals of 0.2 mgl. The algebraic sums of these contours were found and the values contoured. These contoured values were then subtracted from the original gravity contours. The results are shown on the gravity map by light dashed lines. A considerable area in the vicinity of Monk Hill is included inside the 19 mgl contour (the maximum value inside this contour is 19.3 mgl). Moreover the shape of this contour indicates that further smoothing could be accomplished by taking masses to the north or south of Howard Street; however, the profiles do not extend far enough east and west to permit this to be done with any degree of accuracy, and therefore the calculations have not been carried out.

The positions and sizes of the masses which are assumed in order to reproduce the observed data are, to a very great extent, quite arbitrary, and there is an infinite number of distributions which would satisfy the required conditions. However, it is highly probable that the particular distribution chosen above is one of the simplest and therefore is quite justified.

This arrangement of point masses naturally does not correspond to anything in nature, and in order to obtain a more plausible interpretation, a continuous distribution of matter is required; this can be achieved in the following way.

It can be shown that the gravitational field outside a closed surface and resulting from matter within the surface is identical with the field outside the surface produced by a certain distribution of matter over the surface. The surface density of matter at a point Q' on the surface, $\sigma_{Q'}$, must satisfy the relation

$$(\partial U / \partial n)_{Q'} = -2\pi\sigma_{Q'} - \iint_S (1/r^2) \cos \phi \sigma_Q dS$$

where U is the potential at Q' resulting from the mass distribution inside the surface S , n the normal to the surface at Q' , r the distance from Q' to a variable point Q on S , ϕ the angle between the line $Q'Q$ and the normal at Q' , and the integral is taken over the entire surface of S .

If the closed surface consists of an infinite plane completed by another surface at infinity, the integral is zero since ϕ is 90° for the infinite plane, and r is infinite for the curved surface at infinity. Therefore at any point on the plane,

$$(\partial U / \partial n) = -g/\gamma = -2\pi\sigma$$

Mathematically, the mass on the plane corresponding to σ is distributed over an infinitely thin surface with a varying density such that $\sigma = \rho \Delta h$, ρ being the density and Δh the thickness. However, Δh may be taken as a finite thickness h without too much error. Accordingly, for a point mass, the corresponding values of h on a plane at a distance z are

$$\begin{aligned}
 h &= \sigma / \rho = g / 2\pi \delta \rho \\
 &= (1/2\pi\rho)(m/z^2)\cos^3\theta \\
 &= (g_0/2\pi\rho)(z_0/z)^2\cos^3\theta
 \end{aligned}$$

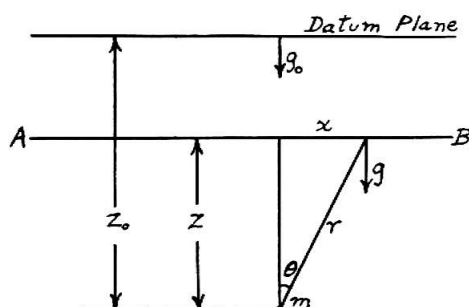


Fig. 2

Since the changes in the measured values of gravity are caused by the difference in density of the basement rocks and the alluvium, the density ρ should be replaced by the density contrast σ . No accurate values of this quantity were available, but 0.5 is probably a reasonable value. Using this value, and substituting $\gamma = 6.67 \times 10^{-8}$, also expressing g_0 in milligals and h in feet, one gets

$$h = 156g_0(z_0/z)^2\cos^3\theta$$

The quantity z may be chosen so that the plane AB is anywhere between the datum plane and the depth z_0 . However the choice is not perfectly arbitrary, since with several point masses the plane AB must be above the shallowest mass, in the present case, above a plane 400 feet below the datum plane (i.e., more than 500 feet above sea level). Also, since the basement outcrops on Monk Hill, h should have a value such that the highest point on the 'swept-up' mass corresponds in elevation to the highest point on Monk Hill.

By trial and error it was found that with a density contrast of 0.5 the best position of AB was 900 feet above sea level. Using a density contrast of 0.3 the best position was 800 feet above sea level. The basement profiles for these two cases, also the curve

for $\sigma = 0.2$, AB 800 feet above sea level, will be found inside the back cover. For comparison, the ground surface and the approximate seismic profile are plotted on the same diagram, together with the positions of the point masses.

CONCLUSIONS

The curve for $\sigma = 0.5$ agrees very well with ground profile and the seismic profile in the vicinity of Monk Hill, but deviates widely from the latter to the west of this area. As lower values of the density contrast are used, the curves approach the seismic profile in the western portion, but give basement elevations above the ground surface at the east end of the curve. Several curves for various values of σ and different elevations of the plane AB were calculated, but it was found that the curve shown for $\sigma = 0.5$ seemed to be most consistent with the data available, both geological and gravitational.

An interesting feature of these curves is that while the seismic profile has a point of inflection approximately midway between El Sereno and Fair Oaks Avenue, all of the gravity profiles have a point of inflection under Raymond Avenue. Each of the curves mentioned above but not shown on the diagram had a point of inflection near this same point. This may indicate that the slope of the basement in this region may be greater than that indicated by the seismic profile.

Although the discrepancy between the gravity and seismic profiles could be explained by postulating a lateral increase in

density of the basement rocks, the highest density being under Monk Hill, there is no geological evidence for such a rapid change in density, and therefore it is felt that such an explanation is highly speculative.

The original gravity contours are slightly elongated towards the northwest and southeast, and the elongation becomes much more pronounced after removal of the effect of the point masses. This may indicate that Monk Hill, as well as the valley to the west, have axes parallel to this direction.

APPENDIX A

Gravity Data for the Monk Hill Area

Stn No.	Elev. (ft)	y (ft)	Time	Gravimeter Reading		Corrections			g (mg1)
				(div)	(mg1)	Drift (mg1)	Elev* (mg1)	Lat. (mg1)	
6d	183.2	+1700	8.51	171.8	17.37	-10.09	12.59	-0.18	19.69
5d	188.0	+2090	9.02	164.9	16.67	-10.07	12.92	-0.22	19.30
4d	189.8	+2450	9.13	160.0	16.18	-10.07	13.04	-0.25	18.90
6d			9.21	171.4	17.33	-10.05	12.59	-0.18	19.69
3d	192.6	+2840	9.29	154.4	15.61	-10.03	13.23	-0.30	18.51
02d	194.3	+3270	9.38	148.0	14.96	-10.01	13.35	-0.34	17.93
2d	196.0	+3590	9.45	143.1	14.47	- 9.99	13.47	-0.37	17.58
1d	204.5	+4150	9.53	132.3	13.38	- 9.99	14.05	-0.43	17.01
6d			10.00	170.6	17.25	- 9.97	12.59	-0.18	19.69
7d	184.6	+1320	10.14	172.5	17.44	- 9.96	12.68	-0.14	20.02
8d	195.0	+ 820	10.24	165.1	16.69	- 9.95	13.40	-0.09	20.05
6d			10.31	170.4	17.23	- 9.95	12.59	-0.18	19.69
10d	80.4	- 675	10.45	216.1	21.85	- 9.94	5.52	+0.07	17.50
11d	62.2	-1135	10.54	225.0	22.75	- 9.94	4.27	+0.12	17.20
6d			11.03	170.2	17.21	- 9.93	12.59	-0.18	19.69
12d	57.2	-1325	11.11	227.0	22.95	- 9.93	3.93	+0.14	17.09
13d	36.3	-1950	11.23	240.0	24.26	- 9.92	2.49	+0.20	17.03
14d	23.8	-2600	11.30	249.9	25.25	- 9.91	1.64	+0.27	17.25
6d			11.39	170.0	17.19	- 9.91	12.59	-0.18	19.69
5b	151.2	+1800	8.56	184.8	18.68	- 9.89	10.39	-0.08	19.10
6d	183.2	+1700	9.03	169.5	17.14	- 9.87	12.59	-0.18	19.68
4b	172.0	+1380	9.10	174.3	17.62	- 9.85	11.82	-0.14	19.45
5b			9.20	184.2	18.62	- 9.83	10.39	-0.08	19.10
1b	214.7	+4340	9.29	124.7	12.61	- 9.82	14.75	-0.45	17.09
2b	204.1	+3280	9.35	139.5	14.10	- 9.82	14.02	-0.34	17.96
3b	181.4	+2090	9.44	165.4	16.72	- 9.81	12.46	-0.22	19.15
5b			9.53	184.0	18.60	- 9.81	10.39	-0.08	19.10
6b	107.4	0	10.02	204.5	20.67	- 9.80	7.38	0.00	18.25
7b	72.8	- 675	10.14	221.7	22.41	- 9.78	5.00	+0.07	17.70
5b			10.21	185.7	18.57	- 9.78	10.39	-0.08	19.10
8b	61.1	-1270	10.28	230.1	23.26	- 9.78	4.20	+0.13	17.81
9b	44.8	-1960	10.35	241.3	24.40	- 9.79	3.08	+0.20	17.89
10b	36.2	-2600	10.42	249.6	25.23	- 9.79	2.49	+0.27	18.20
5b			10.50	185.9	18.59	- 9.80	10.39	-0.08	19.10
6d	183.2	+1700	10.59	169.1	17.10	- 9.81	12.59	-0.18	19.70
5b			11.18	184.3	18.63	- 9.84	10.39	-0.08	19.10

*All elevations corrections on pages 18-20 are positive.
 (For explanation of letters after station numbers see page 20).

APPENDIX A

Gravity Data for the Monk Hill Area (cont'd)

Stn. No.	Elev. (ft)	y (ft)	Time	Gravimeter Reading		Corrections			g (mgl)
				(div)	(mgl)	Drift (mgl)	Elev. (mgl)	Lat. (mgl)	
6c	177.7	+ 825	1.55	173.3	17.54	- 9.71	12.21	-0.09	19.95
5c	157.9	+ 825	2.01	182.6	18.46	- 9.72	10.85	-0.09	19.50
4c	186.7	+2040	2.07	163.1	16.49	- 9.73	12.83	-0.21	19.38
3c	201.2	+3300	2.14	142.2	14.38	- 9.74	13.82	-0.34	18.12
2c	204.3	+3600	2.18	136.9	13.84	- 9.75	14.04	-0.37	17.76
6c			2.25	174.0	17.59	- 9.76	12.21	-0.09	19.95
1c	211.4	+4390	2.34	126.4	12.78	- 9.76	14.52	-0.46	17.08
6d	183.2	+1700	2.42	168.5	17.04	- 9.76	12.59	-0.18	19.69
7c	110.8	+ 75	2.50	203.0	20.52	- 9.76	7.61	-0.01	18.36
6c			2.56	174.0	17.59	- 9.76	12.21	-0.09	19.95
8c	76.0	- 675	3.01	217.6	22.00	- 9.76	5.22	+0.07	17.53
11c	29.7	-2600	3.09	248.5	25.12	- 9.77	2.04	+0.27	17.66
10c	35.3	-2080	3.14	243.0	24.57	- 9.77	2.43	+0.22	17.45
9c	56.2	-1270	3.20	229.1	23.16	- 9.78	3.86	+0.13	17.37
6c			3.28	174.3	17.62	- 9.79	12.21	-0.09	19.95
8e	168.5	+1320	1.09	181.3	18.33	-10.25	11.58	-0.14	19.52
9e	166.0	+ 825	1.19	184.3	18.63	-10.24	11.40	-0.09	19.70
10e	136.9	+ 80	1.26	194.4	19.65	-10.24	9.41	-0.01	18.81
8e			1.32	181.2	18.32	-10.24	11.58	-0.14	19.52
6d	183.2	+1700	1.40	173.3	17.52	-10.24	12.59	-0.18	19.69
11e	102.0	- 735	1.50	204.3	20.65	-10.24	7.01	+0.08	17.50
8e			1.58	181.3	18.33	-10.25	11.58	-0.14	19.52
14e	39.0	-2280	2.09	235.8	23.84	-10.27	2.68	+0.24	16.49
15e	21.8	-2600	2.15	247.9	25.06	-10.28	1.50	+0.27	16.55
13e	74.2	-1315	2.22	216.2	21.86	-10.30	5.10	+0.14	16.80
8e			2.30	181.9	18.39	-10.31	11.58	-0.14	19.52
12e	80.3	-1100	2.38	214.1	21.65	-10.32	5.52	+0.11	16.96
1e	200.1	+4170	2.48	133.7	13.52	-10.32	13.75	-0.43	16.52
2e	189.1	+3570	2.53	145.7	14.73	-10.33	12.99	-0.37	17.02
8e			3.01	182.1	18.41	-10.33	11.58	-0.14	19.52

Gravity Data for the Monk Hill Area (cont'd)

Stn. No.	Elev. (ft)	y (ft)	Time	Gravimeter Reading		Corrections			g (mgls)
				(divs)	(mgls)	Drift (mgls)	Elev. (mgls)	'Lat.' (mgls)	
12e	80.3	-1100	2.38	214.1	21.65	-10.32	5.52	+0.11	16.96
1e	200.1	+4170	2.48	133.7	13.52	-10.32	13.75	-0.43	16.52
2e	189.1	+3570	2.53	145.7	14.73	-10.35	12.99	-0.37	17.02
8e			3.01	182.1	18.41	-10.33	11.58	-0.14	19.52
8e			11.06	202.3	20.45	-12.37	11.58	-0.14	19.52
3e	184.2	+3220	11.13	172.5	17.44	-12.38	12.65	-0.33	17.38
4e	181.2	+2810	11.17	179.1	18.11	-12.38	12.45	-0.29	17.89
5e	179.5	+2450	11.22	186.0	18.80	-12.38	12.33	-0.25	18.50
6e	174.9	+2090	11.26	193.4	19.55	-12.39	12.02	-0.22	18.96
7e	171.9	+1730	11.31	198.7	20.09	-12.39	11.81	-0.18	19.33
5*	83.4	+460	11.38	220.4	22.28	-12.39	5.73	+0.05	15.67
8e			11.45	202.6	20.48	-12.40	11.58	-0.14	19.52
8a	96.3	+1730	12.00	252.8	25.56	-12.40	6.61	-0.18	19.59
5b	181.4	+800	12.07	209.7	21.20	-12.40	10.39	-0.08	19.11
1a	146.5	+1395	12.15	207.1	20.94	-12.41	10.06	-0.15	18.44
2a	123.3	+1430	12.20	220.6	22.30	-12.41	8.47	-0.15	18.21
3a	120.9	+1500	12.27	222.1	22.45	-12.41	8.31	-0.16	18.19
4a	113.8	+1530	12.31	228.0	23.05	-12.41	7.82	-0.16	18.30
5a	98.7	+1570	12.38	239.0	24.16	-12.42	6.78	-0.16	18.36
8a			12.42	253.0	25.58	-12.42	6.61	-0.18	19.59
6a	93.3	+1660	12.48	246.0	24.87	-12.42	6.41	-0.17	18.69
7a	94.5	+1755	12.53	250.7	25.34	-12.42	6.49	-0.18	19.23
14a	102.9	+2040	1.02	266.5	26.94	-12.43	7.07	-0.21	21.37
13a	100.8	+1965	1.08	265.8	26.87	-12.43	6.93	-0.20	21.17
12a	99.0	+1920	1.12	263.1	26.60	-12.43	6.80	-0.20	20.77
11a	97.1	+1875	1.15	261.9	26.48	-12.43	6.67	-0.20	20.52
10a	95.7	+1895	1.20	259.8	26.27	-12.43	6.58	-0.20	20.22
9a	96.5	+1780	1.24	255.6	25.84	-12/43	6.63	-0.19	19.85
8a			1.27	253.1	25.59	-12.43	6.61	-0.18	19.59

(5* is Stn. 5 in Washington Park - see Table below)

Gravity Data for Certain Washington Park Stations.

Stn. No.	Elev. (ft)	y (ft)	Reading** (See page 22)		Reading (Dec. 26) (mgls)	Adjusted Reading (mgls)	Elev. Corr. (mgls)	Lat. Corr. (mgls)	g (mgls)
			(divs)	(mgls)					
5	83.4	-460	11.1	1.12	9.89	9.89	5.73	+0.05	15.67
10	104.0	+75	5.8	0.59		9.36	7.14	-0.01	16.49
20	99.4	+0	2.0	0.20		8.97	6.83	+0.00	15.80

(** - readings corrected for drift only.)

Street Designations.

- | | |
|-------------------|---------------------|
| a - Howard Street | b - Raymond Ave. |
| c - Summit Ave. | d - Marengo Ave. |
| e - Garfield Ave. | f - Washington Park |

- 01 -
APPENDIX B

Table 1 Survey Data for Stations in Washington Park.

Inst.	Stn.	Dist	Bearing	Vert.	Δz	Δx	Δy	x	y	z
Loc.	No.	(ft)	(mag.)	Angle	(ft)	(ft)	(ft)	(ft)	(ft)	(ft)
	10**							87	500	34.2
T.P.1*	10	101	N07 $\frac{1}{2}$ W	0 00'	+ 2.7	+ 13	-105	100	395	36.9
	4	5	N89E	0 00'	- 4.6	0	+ 5	100	400	32.3
	3	106	S15 $\frac{1}{2}$ E	-2 38'	- 9.7	+ 28	- 97	128	298	27.2
	2	204	S15E	-2 42'	-14.4	+ 53	-192	153	203	22.5
	1	297	S15 $\frac{1}{2}$ E	-2 43'	-18.9	+ 78	-281	178	114	18.0
	5	387	S15 $\frac{1}{2}$ E	-2 44'	-23.3	+102	-368	202	27	13.6
	11	213	S38 E	-3 00'	-16.0	+133	-161	233	234	20.9
	12	133	S53E	-2 39'	-11.0	+106	- 75	206	320	25.9
	8	236	N73 E	-3 39'	-19.7	+227	+ 71	327	466	17.2
T.P.2*	8	138	N76 $\frac{1}{2}$ E	0 00'	+ 4.7	-134	- 33	193	433	21.9
	7	89	N77 $\frac{1}{2}$ E	-0 04'	- 5.8	+ 86	+ 20	279	453	16.1
	13	46	N79 $\frac{1}{2}$ E	-0 02'	- 5.7	+ 45	+ 9	238	442	16.2
	29	100	S23E	-1 52'	- 3.0	+ 45	- 93	238	340	13.9
T.P.3*	7	66	N31 $\frac{1}{2}$ W	0 00'	+ 1.9	+ 34	- 56	313	397	18.0
	17	33	S76 $\frac{1}{2}$ W	0 00'	- 5.3	- 31	- 8	282	389	12.7
	16	9	N63 W	0 00'	- 4.7	+ 9	+ 4	322	401	13.3
	15	69	N72 $\frac{1}{2}$ W	0 00'	- 4.5	+ 66	+ 21	379	418	13.5
	18	64	S31E	0 00'	- 5.5	+ 34	- 55	347	342	12.5
T.P.4*	18	53	N76 $\frac{1}{2}$ W	0 00'	+ 4.9	+ 51	- 13	398	329	17.4
	19	6	N20 $\frac{1}{2}$ W	0 00'	- 5.0	- 2	+ 6	396	335	12.4
	21	45	S26 W	0 00'	- 5.7	- 20	- 40	378	289	11.7
	28	95	S24 $\frac{1}{2}$ W	-1 19'	- 7.9	- 39	- 86	359	243	9.5
T.P.5*	28	51	N66 $\frac{1}{2}$ E	0 00'	+ 6.2	- 47	- 20	312	223	15.7
	31	4	S14E	0 00'	- 5.7	+ 1	- 4	313	219	10.0
	30	48	N33 W	0 00'	- 4.3	- 26	+ 39	286	262	11.4
	32	118	S32 $\frac{1}{2}$ E	-1 35'	- 8.6	+ 63	-100	375	123	7.1
	33	111	S73E	-2 16'	- 9.7	+106	- 33	418	190	6.0
	14	80	S31 W	0 00'	- 2.2	- 42	- 69	270	154	13.5
T.P.6*	14	39	S37 W	0 00'	+ 4.6	+ 24	+ 31	294	185	18.1
	34	57	S15 $\frac{1}{2}$ E	-2 13'	- 8.0	+ 15	- 55	309	130	10.1
T.P.7*	14	124	N37E	-0 09'	+ 6.1	- 75	- 99	195	55	19.6
	36	70	N44E	0 00'	- 5.0	+ 49	+ 51	244	106	14.6
	35	102	N70 $\frac{1}{2}$ E	-2 19'	- 8.9	+ 96	+ 35	292	90	10.7
	5	27	S16E	-0 12'	- 6.0	+ 8	- 26	203	29	13.6
T.P.8*	10	188	N88W	0 00'	+ 2.1	+188	- 7	275	493	36.3
	6	41	S74 W	0 00'	- 4.1	- 40	- 11	235	482	32.2
	20	164	N75 $\frac{1}{2}$ E	0 00'	- 6.8	+158	+ 42	433	535	29.5
T.P.9*	21	63	S58 E	+4 24'	- 3.8	- 54	+ 33	324	322	7.9
	27	86	N44 $\frac{1}{2}$ W	0 00'	- 2.5	- 60	+ 62	254	384	5.4
	26	28	N48 $\frac{1}{2}$ W	0 00'	- 5.1	- 21	+ 18	303	340	2.8
	25	30	S59 E	0 00'	- 6.0	+ 26	- 15	350	307	1.9
T.P.10*	25	106	N64 W	0 00'	+ 3.8	+ 96	- 45	446	252	5.7
	24	40	N62W	0 00'	- 4.9	- 36	+ 18	410	280	0.8
	23	25	S15 $\frac{1}{2}$ E	0 00'	- 5.5	+ 6	- 24	452	238	0.2
	22	85	S12 E	0 00'	- 5.7	+ 19	- 83	465	179	0.0
	21	75	N66 W	+7 41'	+ 6.0	- 69	+ 29	377	291	11.7
T.P.11*	8	2	N85W	0 00'	+ 4.6	0	+ 2	327	468	21.8
	9	45	N77 $\frac{1}{2}$ E	+0 45'	- 2.0	+ 43	+ 8	370	476	19.8

* Coordinates refer to T.P. (Turning Point)

** Coordinates chosen arbitrarily.

All elevations are relative to a datum plane 970' above sea level. x axis is east-west, y axis north-south

APPENDIX B.

Table 2. Gravity Data for Stations in Washington Park

Stn. No.	Date	Time	Meter Rdg. (div)	Drift Corr. (div)	g (div)	Stn. No.	Date	Time	Meter Rdg. (div)	Drift Corr. (div)	g (div)
1	Oct.	9.10	10.5	-0.5	10.0	1	Dec.	10.53	12.1	-2.1	10.0
2	26	9.22	9.8	-0.6	9.2	13	2	11.07	15.9	-2.0	13.9
3		9.26	8.4	-0.7	7.7	8		11.14	13.4	-2.0	11.4
4		9.31	6.7	-0.8	5.9	7		11.17	14.8	-1.9	12.9
1		10.17	11.4	-1.4	10.0	9		11.22	10.7	-1.9	8.8
						15		11.32	13.3	-1.8	11.5
1	Oct.	1.48	15.0	-5.0	10.0	1		11.47	11.7	-1.7	10.0
11	27	1.57	13.3	-4.9	8.4						
12		2.02	11.9	-4.8	7.1	1		2.13	14.1	-4.1	10.0
1		2.32	14.5	-4.5	10.0	18		2.20	17.5	-4.2	13.3
						17		2.25	19.3	-4.2	15.1
1	Dec.	8.38	10.7	-0.7	10.0	16		2.29	18.6	-4.2	14.4
14	2	8.43	13.1	-0.7	12.4	30		2.35	18.4	-4.3	14.1
34		8.48	14.3	-0.8	13.5	31		2.43	18.1	-4.4	13.7
32		8.53	14.5	-0.8	13.7	1		2.48	14.4	-4.4	10.0
1		8.58	10.8	-0.8	10.0						
						5		2.55	15.6	-4.5	11.1
1		9.29	12.2	-2.2	10.0	1		2.58	14.5	-4.5	10.0
36		9.33	13.5	-2.1	11.4						
35		9.39	14.7	-2.1	12.6	11		3.03	13.2	-4.4	8.8
28		9.44	16.0	-2.1	13.9	12		3.07	11.6	-4.3	10.0
33		9.48	16.7	-2.1	14.6	1		3.34	13.9	-3.9	10.0
19		9.52	13.9	-2.0	11.9						
1		10.10	11.9	-1.9	10.0	6		3.42	7.1	-3.9	3.2
						20		3.45	5.8	-3.8	2.0
22		10.18	19.5	-2.0	17.5	10		4.14	9.5	-3.7	5.8
23		10.23	20.4	-2.0	18.4	1		4.20	13.6	-3.6	10.0
24		10.27	21.2	-2.0	19.2						
25		10.32	21.9	-2.0	19.9						
26		10.35	22.9	-2.1	20.8						
27		10.40	22.1	-2.1	20.0						
29		10.45	16.3	-2.1	14.2						
1		10.53	12.1	-2.1	10.0						

APPENDIX B.

TABLE 3.

Data for the Least-Squares Determination of the Density

Station Number	x (feet)	y (feet)	z (feet)	g (div)	c_i (div)
1	178	114	18.0	10.0	-0.5
2	153	203	22.5	9.2	0.3
3	128	298	27.2	7.7	0.4
4	100	400	32.3	5.9	0.4
5	202	27	13.6	11.1	-0.9
6	235	482	32.2	3.2	-0.4
7	279	453	16.1	12.9	-0.4
8	327	466	17.2	11.4	-0.3
9	370	476	19.8	8.8	-0.3
10	87	500	34.2	5.8	0.2
11	233	234	20.9	8.6	0.0
12	206	320	25.9	7.2	0.5
13	238	442	16.2	13.9	-0.1
14	270	154	13.5	12.4	0.4
15	379	418	13.5	11.5	-1.0
16	322	401	13.3	14.4	0.7
17	282	389	12.7	15.1	0.3
18	347	342	12.5	13.3	0.2
19	396	335	12.4	11.9	-0.1
20	433	535	29.5	2.0	0.2
22	465	179	0.0	17.5	0.2
23	452	238	0.2	18.4	0.3
24	410	280	0.8	19.2	0.2
25	350	307	1.9	19.9	0.1
26	303	340	2.8	20.8	0.2
27	264	384	5.4	20.0	-0.1
28	359	243	9.5	13.9	0.1
29	238	340	13.9	14.2	-0.2
30	286	262	11.4	14.1	-0.2
31	313	219	10.0	13.7	-0.5
32	375	123	7.1	13.7	-0.1
33	418	190	6.0	14.6	0.3
34	309	130	10.1	13.5	0.3
35	292	90	10.7	12.6	-0.1
36	244	106	14.6	11.4	0.1

$$\begin{aligned}
 \sum x_i &= 133,871.8 & \sum y_i &= 123,385.1 & \sum z_i &= 4,960.27 \\
 \sum x_i^2 &= 10,243 & \sum y_i^2 &= 3,318,131 & \sum x_i y_i &= 3,041,009 \\
 \sum y_i^2 &= 10,420 & \sum y_i z_i &= 3,716,608 & \sum x_i z_i &= 128,242.3 \\
 \sum z_i^2 &= 507.9 & \sum z_i^2 &= 10,275.69 & \sum y_i z_i &= 169,840.8 \\
 \sum g_i &= 433.8 & N &= 35 & \sum c_i^2 &= 4.88
 \end{aligned}$$

APPENDIX B

Least-squares Determination of k.

Substituting the data on the preceding page in equations

(4), page 7, the following set of equations is obtained.

$$35a_{00} + 10243a_{10} + 10420a_{01} - 507.9k = 433.8 \dots (1)$$

$$10243a_{00} + 3318131a_{10} + 3041009a_{01} - 128242.3k = 133871.8 \dots (2)$$

$$10420a_{00} + 3041009a_{10} + 3716608a_{01} - 169840.8k = 123385.1 \dots (3)$$

$$-507.9a_{00} - 128242.3a_{10} - 169840.8a_{01} + 10275.69k = -4960.27 \dots (4)$$

a_{00} is eliminated by dividing Eqn. 1 by 35, and multiplying the result by 10243, 10420, and -507.9 successively, then subtracting the first equation so obtained from Eqn. (2) above, the second from (3), and the third from (4). In this way the following equations result.

$$320444a_{10} - 8478a_{01} + 20398.3k = 6917.1 \dots (2a)$$

$$-8478a_{10} + 614425a_{01} - 18631.7k = -5763.4 \dots (3a)$$

$$20398.3a_{10} - 18631.7a_{01} + 2905.34k = 1334.79 \dots (4a)$$

In the same way a_{10} and a_{01} may be eliminated, the following series of equations being obtained.

$$614201a_{01} - 18092k = -5580.4 \dots (3b)$$

$$-18092a_{01} - 1606.86k = 894.47 \dots (4b)$$

$$1073.94k = 730.09 \dots (4c)$$

Therefore, $k = 0.680$, $b = 1073.94 = 1074$. Substituting these values in the above equations, the following values are obtained for the remaining unknowns: $a_{00} = 25.3$, $a_{01} = 0.0109$, $a_{10} = -0.0214$.

The residuals $c_i^!$ are given by the relation

$$\begin{aligned} c_i^! &= (a_{00} + a_{10}x_i + a_{01}y_i) - (g_i + kz_i) \\ &= 25.3 - 0.0214x_i + 0.0109y_i - 0.680z_i - g_i \end{aligned}$$

The values of x_i , y_i , z_i , and g_i for each station were substituted in this expression, and the values of $c_i^!$ for each station calculated. These values are listed in Table 3, page 23.

REFERENCES

- (1) W. J. Miller: "Geology of the Western San Gabriel Mountains of California", Publications of the University of Southern California at Los Angeles in Mathematical and Physical Sciences, Vol. 1, No. 1 (1934).
- (2) J. A. Legge, Jr.: "A proposed Least Square Method for the Determination of the Elevation Factor", Geophysics, Vol. 9, 175 (1944).
- (3) R. A. Fisher: "Statistical Methods for Research Workers", (Stechart Co.), 8th Ed., p.42.

TRANSMISSION OF SHOT IMPULSES
IN SHALLOW WATER

Thesis by
Lloyd Philip Geldart

In Partial Fulfillment of the Requirements
For the Degree of
Geophysical Engineer

California Institute of Technology
Pasadena, California

1949

ACKNOWLEDGMENTS

The author wishes to express his gratitude to the United Geophysical Company, Pasadena, for providing the opportunity to carry out the work described in the following report, and also for permission to write this report.

The writer is grateful also to Dr. R. A. Peterson under whose direction the work was carried on, and also to Mr. Robert Day with whom the author collaborated in the construction and testing of the apparatus.

ABSTRACT

The properties of various types of waves set up by underwater explosions is discussed from the viewpoint of their application in locating shot points in seismic work carried on over water. The construction of the audio amplifiers and filters used to record these waves is described, together with the results of a preliminary check of their performance.

TABLE OF CONTENTS

<u>PART</u>	<u>TITLE</u>	<u>PAGE</u>
I	INTRODUCTION	1
II	TRANSMISSION OF SOUND IN WATER AND IN THE BOTTOM LAYERS	2
III	CONSTRUCTION OF APPARATUS	8
IV	EXPERIMENTAL PROCEDURE AND RESULTS	8
V	CONCLUSIONS	11
VI	BIBLIOGRAPHY	12

INTRODUCTION

In carrying out seismic exploration on water, one of the problems encountered is the accurate location of the shot points. At present this is usually done by means of sextant observations of shore targets, the positions of the targets being determined by a survey crew on shore.

Early in 1948, the United Geophysical Company, Pasadena, began development work on a project aimed at adapting the methods of radio-acoustic ranging to the determination of shot positions in water work, and the author was privileged to assist in this work during the spring term of 1948.

In radio-acoustic ranging, a radio transmitter is mounted on a buoy, the position of which is determined by a survey crew on shore. Impulses from the shot cause the transmitter to send out a signal which is received and recorded on the recording boat. Because of the high velocity of the radio wave, the time interval between the firing of the shot and the reception of the radio signal represents the time required for the impulse to travel from the shot point to the buoy. Hence the distance between the shot point and the buoy can be calculated if the velocity and ray path are known. By using two or more buoys the position of the shot can be found.

The original plans for the work described in this report called for the construction of suitable apparatus and the testing of the equipment under actual field condit-

ions. However, in June, 1948, the United Geophysical Company discontinued the development work temporarily, and therefore this report is necessarily incomplete.

TRANSMISSION OF SOUND IN WATER AND IN THE BOTTOM LAYERS

The electrical circuits involved in radio-acoustic ranging do not present any new problems, so that the chief difficulties which might be encountered are those connected with the transmission of sound impulses in water and in the upper layers of the bottom formations. The pulses arriving at the buoy may be any of the following types: (1) direct waves travelling entirely in the water without reflection, (2) waves travelling all the way in the water but reflected one or more times at the surface and the bottom, (3) waves which have been refracted so that part of their path is along the interface between the water and the bottom, (4) waves similar to (3) but which have travelled along the boundaries between lower formations.

Each of these wave types will have a different velocity, and therefore in order to determine the distance the transmitter must be designed so that it will be actuated by one type only, or it must operate for a certain interval after being triggered by the first arrival, and during this interval it must transmit all of the pulses received. In the latter case determination of the distance involves the identification of one or more of the pulses on the record, and therefore is essentially a problem in interpretation.

Because of the different dispersions in each medium, the frequency spectra of the various wave types will be different, and in principle it should be possible to design filters so that the radio transmitter will be actuated by only one of the wave types. This would be a desirable feature since it would eliminate the necessity of interpreting the records at each shot point. Whether or not this will be possible depends upon the relative frequencies and intensities of the waves, and therefore a brief summary of the general characteristics of each type is given below.

Variations of the velocity in water will determine the paths of the waves travelling solely in water. These variations of the velocity depend upon several factors, the most important being changes in temperature, pressure, and salinity. The velocity is given by the formula $V = \sqrt{\gamma/\rho C}$ where γ is the ratio of the specific heats, ρ the density, and C the compressibility. Using this relation and measured values of γ , ρ , and C , it is found that

$$\partial V/\partial T \approx 5 \text{ meters/sec/}^\circ\text{C at } 0^\circ\text{C}$$

$$\approx 2 \text{ meters/sec/}^\circ\text{C at } 30^\circ\text{C}$$

$$\partial V/\partial s \approx 1.5 \text{ meters/sec/\% at } 0^\circ\text{C}$$

$$\approx 1.0 \text{ meters/sec/\% at } 30^\circ\text{C}$$

$$\partial V/\partial h \approx 0.081 \text{ meters/sec/meter,}$$

s being the salinity in %, and h the depth in meters.

Since the velocity at 15°C is approximately 1500 meters/second, the variation with depth will be negligible for depths less than one or two hundred meters. Data given

by Sverdrup and Fleming (1) show that, for the region off the coast of Southern California during the period March-July, 1937, the salinity was between 33.4 and 33.7‰ in the top fifty to seventy meters, after which it increased more or less uniformly to 34.1-0.2‰ at about 200 meters. Thus, over a period of months and for depths up to 200 meters, the salinity changed by less than 2‰; hence the velocity changes resulting from this factor are probably small in general.

The data given by Sverdrup and Fleming showed that for the same area and for the same period, the temperature of water near shore decreased rapidly during the top few meters from 17-20°C to about 10°C around 50 meters depth, then decreased approximately uniformly to 7°C at 1500 meters. About twenty miles off shore, the temperature was constant at 14°C for the first 80 meters, then dropped very rapidly to 11°C at about 110 meters, after which it decreased uniformly to 6°C at 500 meters. Thus temperature changes can be expected to produce the largest changes in velocity, partly because of the large temperature gradients, and partly because of the relatively high rate of change of velocity with temperature.

In general the velocity will decrease with depth in the upper 500 meters as a result of the decrease in temperature. However in the top 100 meters or so the velocity frequently increases with depth, sometimes as a result of a temperature inversion, sometimes as a result of the pressure increase in an isothermal layer.

Variations in the velocity, whether on a large scale

as discussed above or local variations produced by small changes in temperature or salinity, bubbles, suspended matter, etc., cause the path of the waves to be curved, the curvature being greater, the greater the rate of change of velocity. This curvature, together with a relatively high attenuation due to scattering, restricts the maximum distance at which the direct unreflected wave can be observed. Thus, Worzel and Ewing (2) found that in an isothermal layer the maximum distance at which the direct wave could be observed was about one and one half miles. Since the distances involved in seismic work would usually be greater than this, the direct wave will be absent in most cases. Consequently the only waves which have a path entirely in water will be those which have undergone one or more reflections at the surface and bottom; these will be designated as water waves henceforth.

Worzel and Ewing (loc. cit.) have investigated the water waves experimentally, and Pekeris (3) has derived a theory of propagation of explosive impulses in shallow water. In general, the theoretical and experimental results are in good agreement. The most important results may be summarized as follows. If the shot is located in shallow water, the waves undergo dispersion, whether the receiver is in shallow or deep water. No dispersion occurs if the shot is in deep water. The amount of dispersion is a function of the depth of water, the distance between shot point and receiver, and the material in the surface layer of the bottom; the dispersion is independent of the size and depth of the shot. The

water waves contain frequencies from about 50 cycles/sec up to 10 kilocycles/sec and above, the attenuation being higher for the high frequencies. The dispersion follows the relation

$$(V_0 - V)/V = C/\nu^2$$

where V is the velocity for the frequency ν , V_0 the velocity for the highest observed frequency, and C a constant which varies inversely as the square of the depth of water. C is essentially positive so that the velocity increases with frequency, and consequently the highest frequencies arrive first.

The waves which travel along the interface between the water and the bottom or along deeper interfaces are called ground waves. Considerable information about these waves is given in the references mentioned above, particularly in the paper by Pekeris. He shows that the ground waves precede the water waves for all except very short distances between shot point and receiver. The dispersion is such that the low frequencies arrive first. For each group of waves the energy builds up slowly, reaching a maximum within one or two wave-lengths after the first arrival, then dying out gradually. Usually the ground wave has considerable energy even after the arrival of the water wave. Most of the energy in the ground wave is concentrated in the frequency range from 10 to 30 cycles/second, although frequencies as high as 100 cycles/second have measurable intensity.

Thus, the first arrivals are ground waves with frequencies in the range 10-20 cycles/second; these reach their

maximum amplitudes after an interval of one or two periods, then decrease slowly in intensity, at the same time increasing in frequency. Before the ground waves have died out, the water waves arrive, the high frequencies coming first and building up very rapidly to maximum amplitude. From this point on, the frequency of the water wave decreases while that of the ground waves increases. Eventually the two coincide at a frequency which is of the order of 70-80 cycles/second, depending upon the depth of water and the structure of the bottom; Pekeris calls this the Airy frequency, and shows that after it has been reached, the frequency of the combined waves remains constant while the amplitude decreases.

This summary of the properties of the various waves resulting from an underwater explosion shows that it should be possible to design a circuit so that it would be actuated by the water waves only, provided that the normal noise level in the high frequency range is low compared with the signal intensity in the same range. The most important advantages of using the water waves instead of the ground waves are: (1) the initial amplitude of the water waves builds up much more rapidly, thereby furnishing a more definite triggering pulse, (2) simplified amplifier and filter design, (3) in general the velocity in water would be more uniform over a considerable area than the velocity in the bottom, thus simplifying the determination of distances.

CONSTRUCTION OF APPARATUS

The purpose of the experimental work was to construct apparatus for recording water waves and to test the apparatus under field conditions. However, lack of time permitted only the construction of amplifiers and a rough preliminary check of their characteristics.

The recording apparatus consisted of a thirteen-trace oscillograph, only two of the channels being used. Two identical four stage audio amplifiers were constructed with a variable filter between the first and second stage. The amplifier and filter circuits are shown in Fig. 1, page 9, and the overall amplifier response for each of the three filter settings is shown in Fig. 2, page 10.

The oscillograph and amplifier, along with a short wave radio receiver for obtaining the time break, were mounted on a trailer, together with the necessary batteries and accessories. The tests were made on the Dos Pueblos Ranch, about 19 miles west of Santa Barbara on June 9, 1948.

EXPERIMENTAL PROCEDURE AND RESULTS

Gogolick, Wianco, and Bologna types of hydrophones were used. A life raft was moored 400 feet off shore in about ten feet of water, and the hydrophones suspended from the life raft at a depth of eight feet.

Two water parties were working between three and ten miles off shore, and attempts were made to record waves from shots set off by these parties. However, troubles developed in the radio receiver and in the timing moter circuit, and as

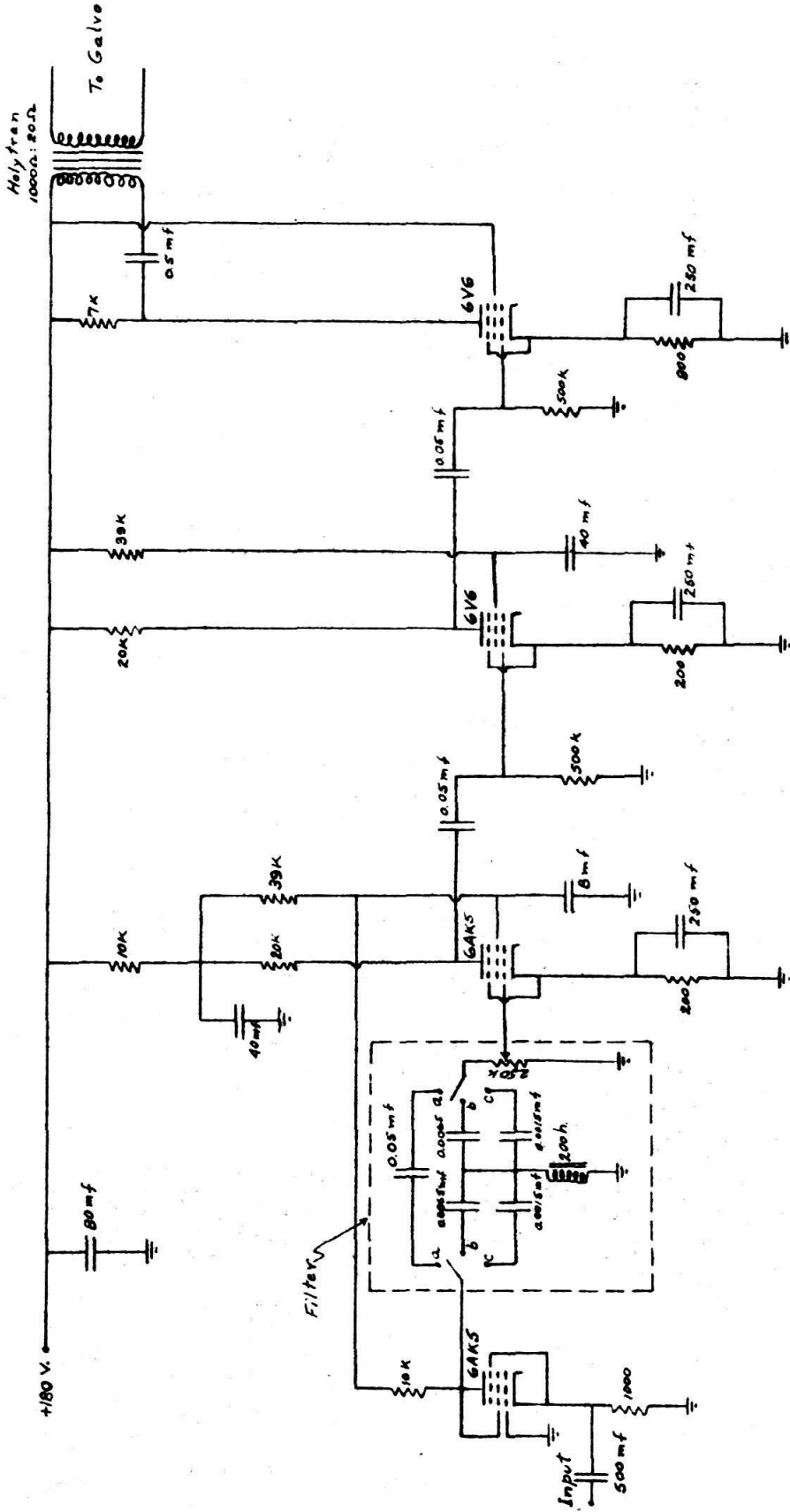


FIG. 1. amplifier circuit.

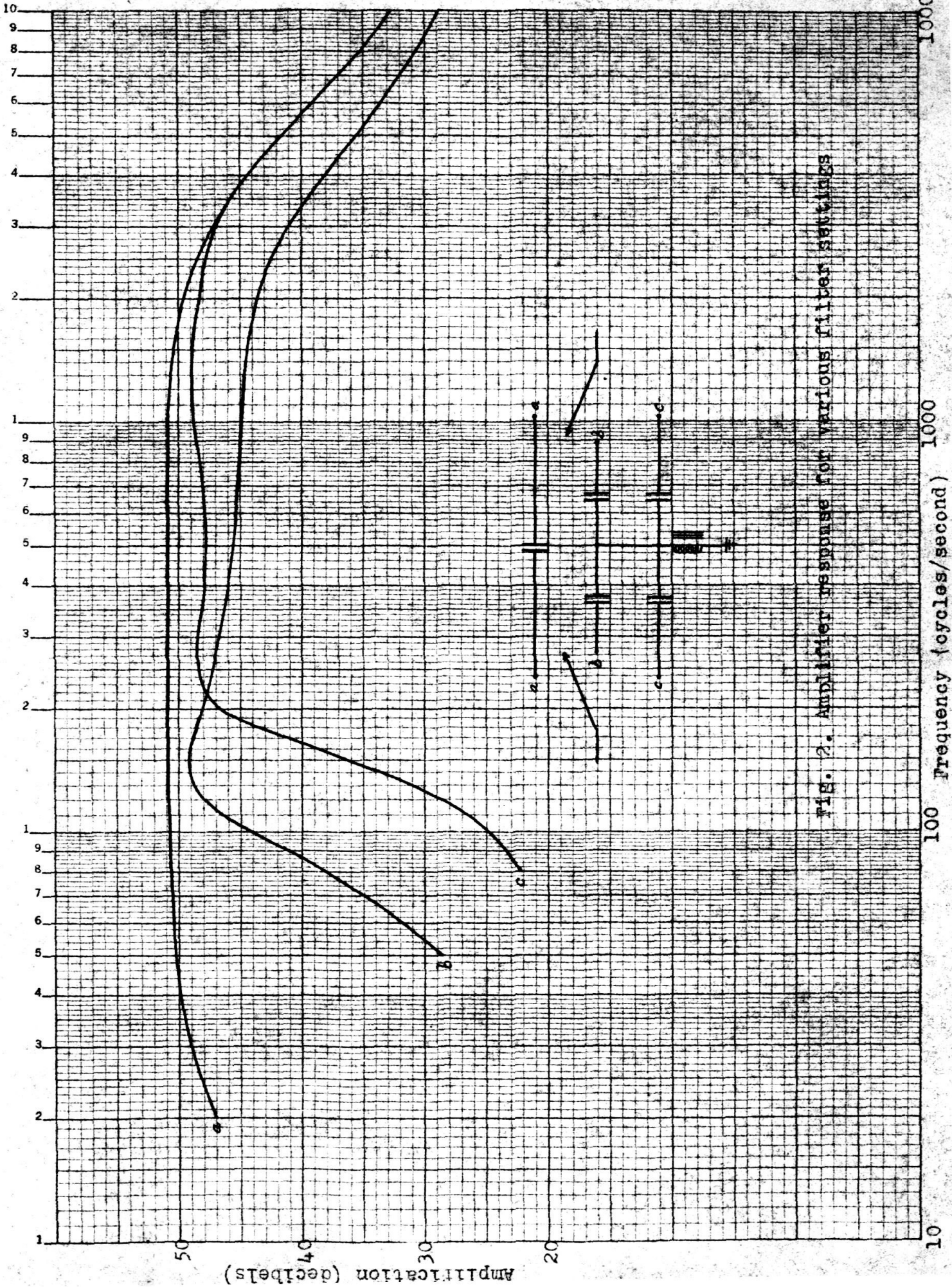


FIG. 2. Amplifier response for various filter settings

a result only seven imperfect records were obtained.

The records were of such poor quality that no attempt was made to analyze them. However it was evident that the frequency and amplitude relationships of the ground and water waves agreed in general with the description given in the preceding sections.

CONCLUSIONS

The results obtained were so meagre and unsatisfactory that no conclusions of any value can be drawn. Nevertheless it is felt that further tests are desirable and may lead to worthwhile developments.

BIBLIOGRAPHY

- (1) Sverdrup, H. V., and Fleming, R. H.: Bulletin of the Scripps Institute of Oceanography (1941), Vol. 4, No. 10, pp. 261-378.
- (2) Worzel, J. L., and Ewing, M.: Geological Society of America, Memoir 27 (1948), pp.
- (3) Pekeris, C. L.: Geological Society of America, Memoir 27 (1948), pp.